Fall 2015

Construction of an Initiated Chemical Vapor Deposition (iCVD) Reactor and Deposition of Polytetrafluoroethylene (Ptfe) Thin Films Using Perfluoro-1-Octanesulfonyl Fluoride as the Initiator

Edgar Kiprop Kosgey

CONSTRUCTION OF AN INITIATED CHEMICAL VAPOR DEPOSITION (iCVD) REACTOR AND DEPOSITION OF POLYTETRAFLUOROETHYLENE (PTFE) THIN FILMS USING PERFLUORO-1-OCTANESULFONYL FLUORIDE AS THE INITIATOR

A Masters Thesis

Presented to

The Graduate College of

Missouri State University

In Partial Fulfillment

Of the Requirements for the Degree

Master of Science, Material Science

By

Edgar Kiprop Kosgey

December 2015

CONSTRUCTION OF AN INITIATED CHEMICAL VAPOR DEPOSITION (iCVD) REACTOR AND DEPOSITION OF POLYTETRAFLUOROETHYLENE (PTFE) THIN FILMS USING PERFLUORO-1-OCTANESULFONYL FLUORIDE AS THE INITIATOR

Department of Physics, Astronomy, and Materials Science

Missouri State University, December 2015

Master of Science

Edgar Kiprop Kosgey

ABSTRACT

Initiated Chemical Vapor Deposition (iCVD) is a surface polymerization technique that is different from other traditional chemical vapor deposition (CVD) techniques. iCVD is carried under a vacuum without the use of solvents, therefore eliminating contaminations. An initiator and a monomer are metered into a vacuum reactor chamber. Inside the reaction chamber is an array of resistively heated filaments and a cooled substrate stage. Monomer species adsorb on to the cooled substrate surface underneath the filament array. The thermal energy from the resistively heated filaments breaks the bonds in the initiator molecule, generating free radicals. These generated free radicals chemisorb to the monomer initiating an in situ free radical polymerization reaction which results in the formation of a polymer thin film. The overall objective of this research was to assemble a custom-built iCVD reactor and use it to grow polytetrafluoroethylene (PTFE) thin films. Perfluoro-1-octanesulfonyl fluoride (PFOSF) was used as the initiator while hexafluoropropylene oxide (HFPO) was used as the monomer. HPFO is well known for its good thermal decomposition. Nichrome filaments were resistively heated at temperature less than 400 ˚C and substrate surface cooled between 10 ˚C and 35 ˚C. Various characterization techniques such FTIR, XPS, SEM, and EDX were performed on as-deposited iCVD PTFE thin films. FTIR spectra of iCVD PTFE showed that the as-deposited iCVD thin films are spectroscopically identical to bulk PTFE.

KEYWORDS: iCVD, PTFE, free radicals, HFPO, PFOSF

This abstract is approved as to form and content

_____

Saibal Mitra, PhD
Chairperson, Advisory Committee
Missouri State University

CONSTRUCTION OF AN INITIATED CHEMICAL VAPOR DEPOSITION (iCVD) REACTOR AND DEPOSITION OF POLYTETRAFLUOROETHYLENE (PTFE) THIN FILMS USING PERFLUORO-1-OCTANESULFONYL FLUORIDE AS THE INITIATOR

By

Edgar Kiprop Kosgey

A Masters Thesis
Submitted to the Graduate College
Of Missouri State University
In Partial Fulfillment of the Requirements
For the Degree of Master of Arts, Material Science

December 2015

Approved:

_____
Saibal Mitra, PhD: Research Advisor

_____
Ridwan Sakidja, PhD: Committee Member

_____
Benjamin Onyango, PhD: Committee Member

_____
Kartik Ghosh, PhD: Committee Member

_____
Julie Masterson, PhD: Dean, Graduate College

ACKNOWLEDGEMENTS

I'm beholden to my graduate research advisor, Dr. Saibal Mitra, for giving me the opportunity to work on this exhilarating research and his incredible support throughout the course of the research. His dedication, motivation, and support saw me through all the stages of my research. This research work has made a difference in my life, and for that, I will be forever thankful to Dr. Mitra for the chance he gave me.

To my thesis committee members, Dr. Ridwan Sakidja and Dr. Benjamin Onyango, thank you for accepting to be part of my thesis committee. You provided me with invaluable and insightful comments on this research and for that I am thankful. Furthermore, I am indebted to the head of Physics, Astronomy, and Material Science Department, Dr. Dave Cornelison, for his encouragement, advice, and support

I would like to give thanks to members of iCVD group in Dr. Mitra's lab, past and present. Special thanks to Sandeep Akkanapragada and Hayley Osman for their tremendous support when I joined the group. Geoffrey Nyauma Manani and Fadayomi Oladeji Taiwo, thank you guys for reading my thesis and providing me with instrumental comments, not to mention the good friendship we have had since our first semester at Missouri State University.

Finally, I would like to acknowledge my whole family in Kenya and USA. Thank you for the encouragement and support. Mr. and Mrs. Sila K. Yego, thank you so much for what you have done for me and my siblings. You have been our pillar of strength and no words can describe how honored and grateful we are to you. To my daughter, Michelle Jebet, you have been a powerful and a wonderful source of my inspiration and energy. To you, I dedicate this thesis.

TABLE OF CONTENTS

LIST OF TABLES

LIST OF FIGURES

CHAPTER 1: INTRODUCTION AND BACKGROUND

Polymeric thin films have a broad range of applications both in research and industrial environment. They have a multitude of applications and a few examples include: surface coating[1,2], surface modification[3], photonics[4,5,6], lithography imaging[7,8,9,10,11,12,13,14], material insulation, microfabrication[15], among others. There are two main techniques used in polymer thin film deposition – Chemical Vapor Deposition (CVD) and spin-on deposition (SOD). In spin-on deposition, a polymer solution is spun on a substrate to produce a thin film and thus it is applicable to various dissolvable polymers. CVD involves the growth of a thin film on a substrate from the use of a monomer building block and an initiator. CVD does not encompass use of solvents. One disadvantage of using solvents is the increase in chances of chemical exposure and also the polymer has to be soluble in the solvent. Not using solvents makes CVD an ideal technique for deposition of polymer thin films. There are several advantages of using a solventless deposition for example initiated Chemical Vapor Deposition (iCVD). These advantages include: thickness control, films of nanoscale sizes can be deposited, excellent conformal coating, and the possibility of coating substrates with complex geometries. This project focuses on the design of a type of chemical vapor deposition technique known as initiated Chemical Vapor Deposition (iCVD) and deposition of polytetrafluoroethylene (PTFE) using perfluo-1-octanesulfonyl fluoride (PFOSF) as the initiator.

1.1 Polytetrafluoroethylene (PTFE)

Polytetrafluoroethylene (PTFE) is a fluoropolymer macromolecule that was discovered serendipitously by a DuPont Company scientist, Roy Plunkett in 1938. There are two categories of fluoropolymers namely partially fluorinated and per fluorinated polymers. Perfluorinated fluoropolymers are homopolymers (polymers that are made up of a single type of monomer units) and copolymers (polymers made up of two different monomers that are linked together and repeated forming a long chain). Figure 1 shows how fluoropolymers have evolved since the late 1930s. PTFE falls under the category of homopolymers.

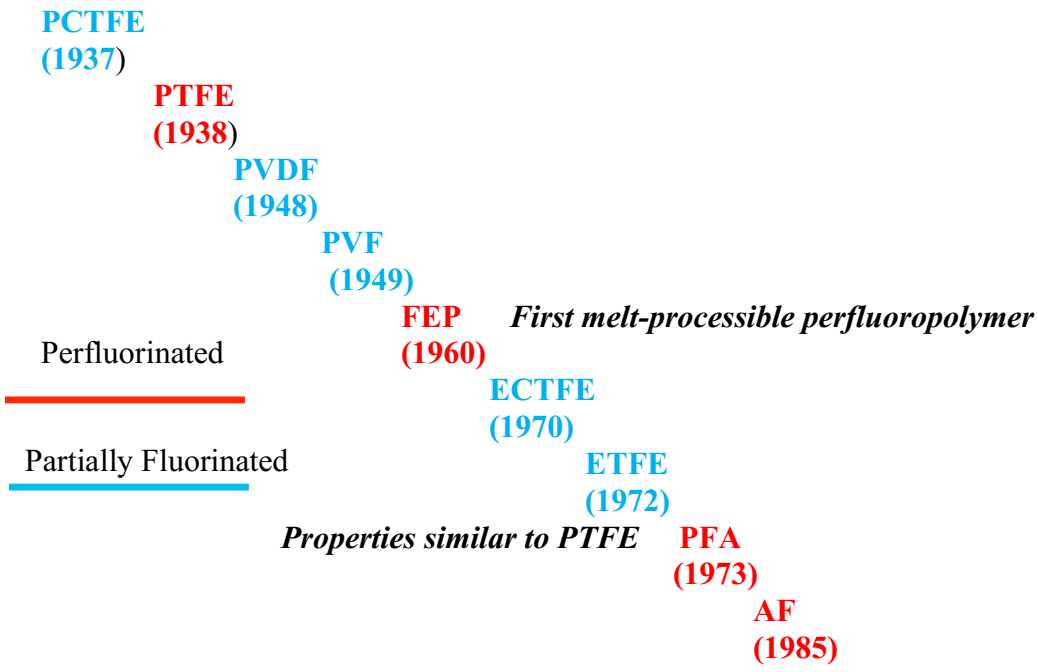

Figure 1: Development of fluoropolymers over a period of time. (Polychlorotrifluoethylne, PCTFE; Polytetrafluoroethylene, PTFE; Polyvinylidene, PVDF; Polyvinyl fluoride, PVF; Fluorinated ethylene-propylene polymer, FEP; Ethylene Chlorotrifluoroethylene polymer, ECTFE; ethylene-Tetrafluoroethylene polymer, ETFE; Perfluoroalkoxy polymer, PFA; Amorphous fluoropolymers, AF)[16]

A crystal structure of PTFE is shown in Figure 2. It is composed of a backbone chain of carbon atoms and two fluorine atoms attached to each carbon atom. Polytetrafluoroethylene has found extensive applications due to its distinctive properties. It is widely known for its ultralow coefficient of friction, hydrophobicity, resistance to chemicals and is completely insoluble in any known solvent. Also as excellent insulator, PTFE has a robust dielectric breakdown potential and a low dielectric constant. Because of its unique properties, PTFE has been considered for applications in insulator materials, capacitor dielectrics, rings and seals for power steering and transmission systems, electrets, cookware coating, and many more industrial applications.

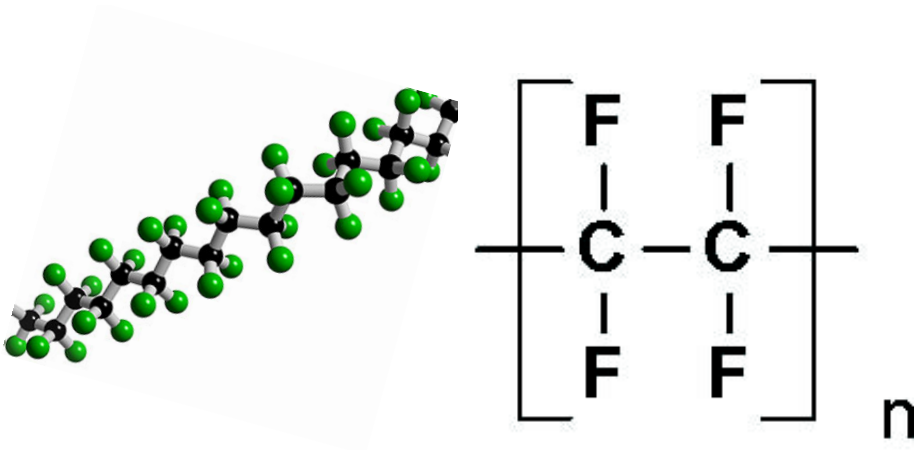

Figure 2: Crystal structure Polytetrafluoroethylene (PTFE).

1.1.1. Hexafluoropropylene oxide (HFPO). In this research, we used Hexafluoropropylene oxide (HFPO) as a monomer. Figure 3 below shows a chemical structure of HFPO. HFPO oxide is a resourceful monomer that can be used in synthesis of polymers and to add functionality to various organic precursors. HFPO is an odorless, colorless, tasteless gas and has a moderately low toxicity. HFPO is used in many

commercial fluoropolymers as a monomer precursor. Its epoxide ring undergoes nucleophilic attack to offer a variation of derivatives.

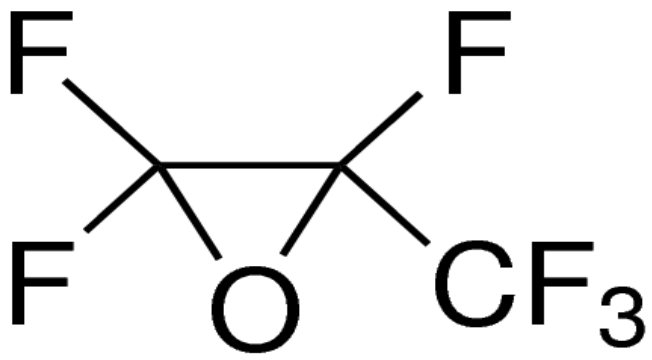

Figure 3: Chemical structure of HFPO

1.1.2 Perfluro-1-octanesulfonyl fluoride (PFOSF). Perfluoro-1-octanesulfonyl fluoride (PFOSF) was used as the initiator in the synthesis of PTFE. PFOSF is a clear colorless liquid. It has a melting point/ freezing point of -15.4 ˚C and an initial boiling point and boiling range of 154 – 155 ˚C. Its relative density and vapor pressure are 1.824 g/cm^3 at 25 ˚C and < 10 mmHg at 20 ˚C respectively. Figure 4 is a chemical structure of perfluoro-1-octanesulfonyl fluoride.

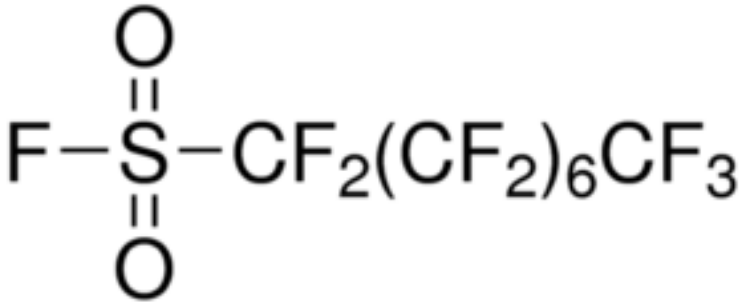

Figure 4: Chemical Structure of Perfluoro-1-Octanesulfonyl Fluoride (PFOSF)

1.2. Physical Vapor Deposition (PVD)

Physical vapor deposition (PVD) is a family of coating processes used to deposit thin layers of solid material on a substrate surface usually in the order of nanometers (nm) to several micrometers (μm). All PVD processes are carried out in a vacuum or partially vacuum environmental and consist of three fundamental stages; (1) material from a solid target is vaporized through direct heating, ablated by plasma or applying a voltage, (2) vaporized material is transported to the substrate surface, and (3) condensation of the vaporized material on the surface of the substrate to produce thin films. Diverse PVD techniques employ the same three fundamental processes but vary in the way the materials are generated and deposited on the substrate. PVD has diverse industrial applications which include fabrication of microelectronic devices, electrodes for batteries and cells, conductive coatings, optical coating, surface modification. Below are two types of PVD techniques discussed in detail.

1.2.1 Pulsed-Laser Deposition (PLD). Pulsed-Laser Deposition (PLD) is an example of a PVD technique that has gained a lot of attention lately because of its ease of use and the ability to deposit materials that are virtually congruent i.e. the ablated species show almost similar stoichiometry as the target material[17]. A typical setup for pulsed-laser deposition is shown in Figure 5. Inside an ultrahigh vacuum (UHV) chamber is the target. Typically, an excimer laser (Lambda Physick) with KrF radiation (wavelength, l =248 nm) that produces high-power pulses is used to ablate materials from the target surface. The laser is focused into the UHV chamber by the use of a set of mirrors. The target is struck at an angle by the high-power and focused laser beam. Material (atoms

and ions) ablated from the target are deposited on the surface of a substrate attached to a surface parallel to the target surface. The distance between the target and the substrate can be varied accordingly.

PLD is a versatile technique whereby thin films of various materials such as polymers, metal oxides, nitrides, and carbides can be deposited. In PLD, various parameters such laser fluence, duration and repatriation rate of the pulse, substrate-to-target distance, substrate temperature, background pressure and gas etc. can be altered which in turn influences the film growth and properties. Furthermore, by introducing oxygen into the vacuum chamber, PLD is particularly suitable for deposition of high-quality oxides. This technique has been observed to not only grow thin films, but also to deposit different nanostructures for example zinc oxide (ZnO) nanowires.

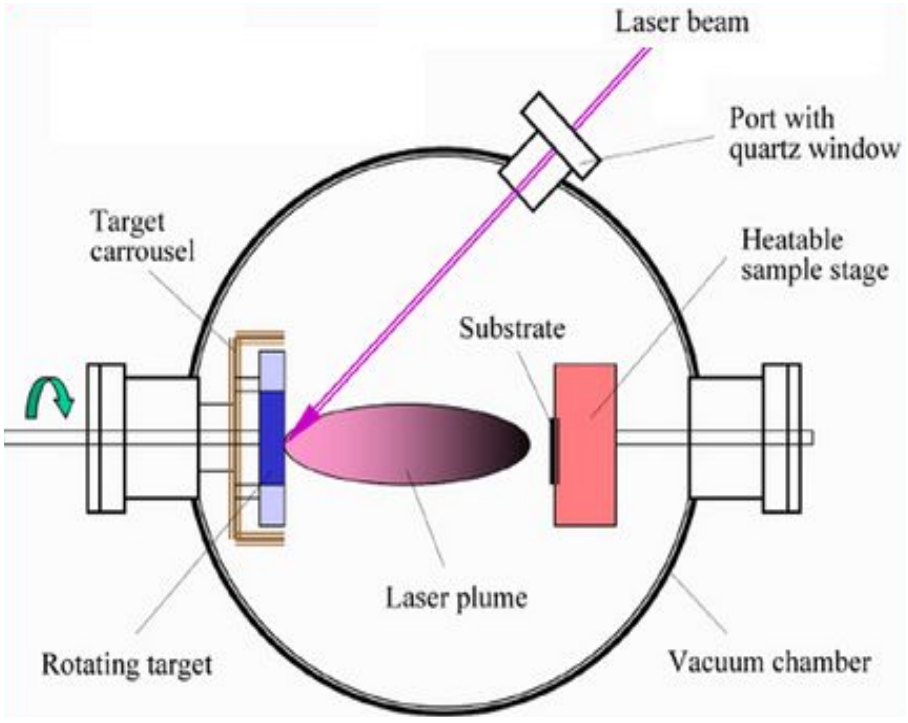

Figure 5: A schematic representation of a typical Pulsed-Laser Deposition (PLD) set-up [18].

1.2.2. Sputtering. Sputtering is an example of a physical vapor deposition (PVD) technique. In sputtering, a target material and a substrate are positioned appropriately inside a vacuum chamber. A voltage is applied across the target material (cathode) and the anode where the substrate is placed. A sputtering gas, typically a heavy inert gas for instance Argon (Ar) is introduced into the vacuum chamber. Figure 6 below shows a typically schematic diagram of a DC plasma sputtering system. A plasma plume is generated through ionization of the sputtering gas. The heavy ionized atoms are accelerated to the target material bombarding it at high velocities[19]. Materials are ablated from the target and deposited on the surface of the substrate.

Sputtering technique has various advantages such as the ability to coat large areas uniformly, high temperatures are not required and therefore alloys and compounds can be sputtered, and diffusive spreading method can be applied thus can coat around corners of substrates.

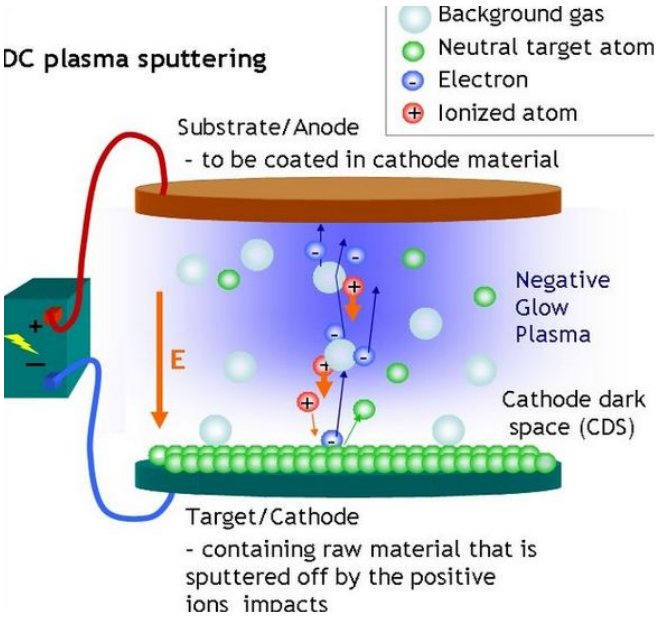

Figure 6: Schematic diagram of a DC plasma sputtering system [20].

1.3. Chemical Vapor Deposition (CVD)

Chemical Vapor Deposition (CVD) is a technique in which thin films are deposited from a vapor through a chemical reaction. A thin film is deposited on a substrate surface on or near a heated surface. In 1879, J. Ogier published the first paper about deposition of solid material through a gaseous phase chemical reaction[21]. In his paper, Ogier discusses thermal decomposition of silicon containing gaseous material to produce thin films of hydrogen containing amorphous silicon[20]. During the early 1960s, the first papers with the phrase "chemical vapor deposition" emerged.

These papers discussed deposition of tungsten films on a heated substrate surface from WF_6. Later on, papers discussing the use of radio-frequency discharge or "plasma" to deposit silicon, silicon oxide (SiO_x) and silicon nitride (SiN_x) were published. CVD has become a popular deposition technique over the years in both industrial and research environments. Figure 7 shows the amount of publications discussing chemical vapor deposition techniques from 1960 to 2010: it depicts a steady increase over the years in publications about chemical vapor deposition (CVD) techniques. There have been more research and publication since the year 2010 to the present. This show how CVD has gained popularity in the both research and industry. Chemical vapor deposition has a wide range of applications in the industry. It has been used to coat a variety of applications for instance high temperature and erosion protection, wear and corrosion resistance, sensors, integrated circuits, optoelectronics (in the semiconductor industry). Also, CVD has been used to produce ceramic composites for example C-C, C-Si carbides, and silicon carbide-silicon carbide composites.

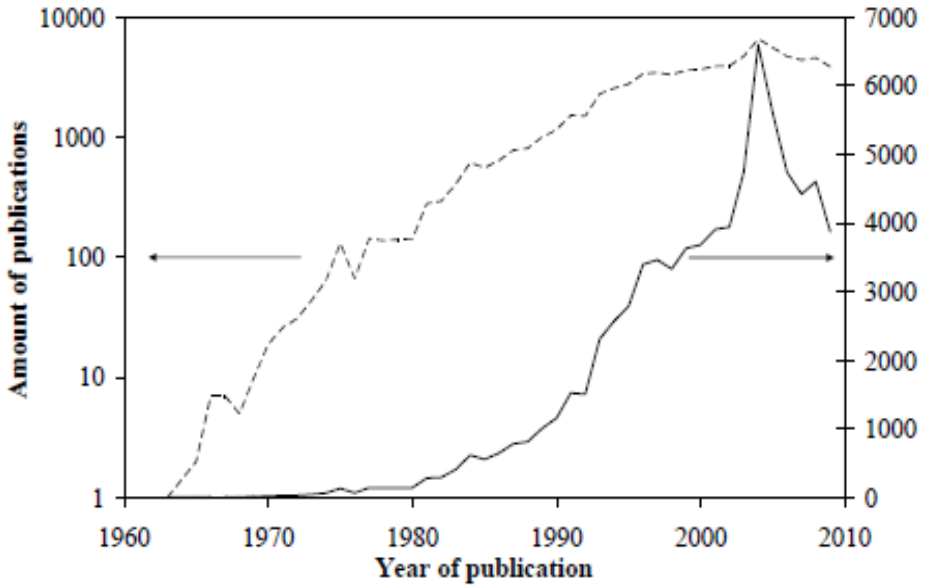

Figure 7: The number of publications discussing chemical vapor deposition (CVD) techniques since 1960 to 2010[22].

In an archetypal CVD, deposition process occurs inside a reaction chamber whereby gaseous reactants are metered into vacuum reactor chamber. When the gaseous reactants come in contact with a heated surface, a chemical reaction takes place. Below is a characteristic chemical reaction inside a CVD reactor:

Gaseous reactants → Solid material + Gaseous products

Figure 8 shows the phases of a typical chemical vapor deposition reaction mechanism. It begins with a mass transport of gaseous reactants into a reaction chamber. Inside the reaction chamber, gas precursors are heated up producing radicals in the gas phase. The radicals then move towards the surface of the substrate on which they are adsorbed. The radicals chemically react with the surface of the growing film. Once it reacts with the surface of the growing film, the radicals are incorporated into the film and

the effluents are removed from the reaction chamber by vacuum pump and through an exhaust system.

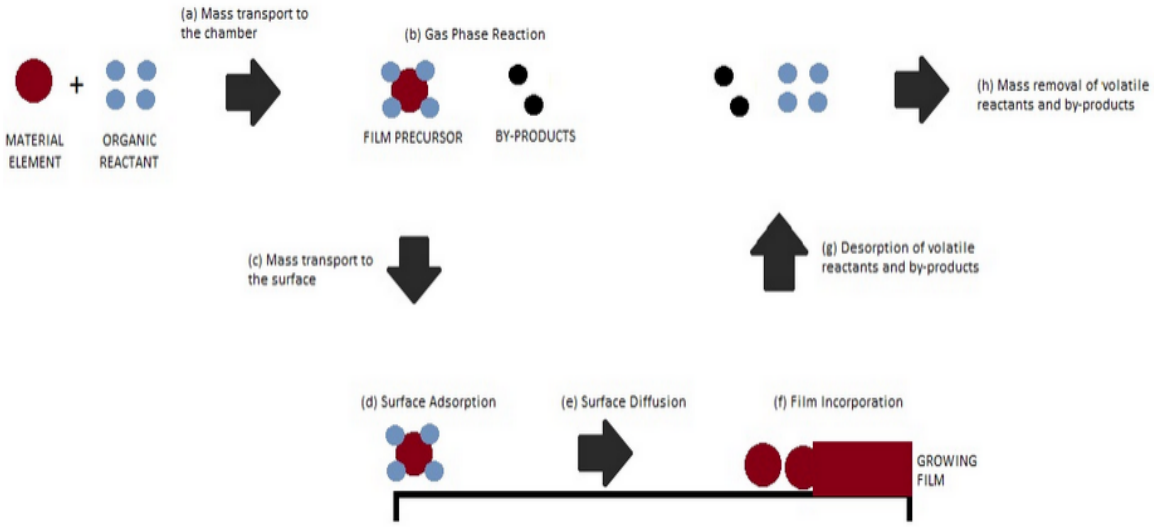

Figure 8: A chemical vapor deposition (CVD) reaction mechanism process [23].

By varying different experimental parameters in a CVD process such as substrate type, substrate temperature, heated surface temperature, reactor pressure, composition of the gas mixture, etc., solid materials/thin films of various properties can be grown. The following are a few characteristics of CVD technique: the ability to grow coatings of uniform thickness and properties, conformal coatings on substrates of complex geometries[24], and the possibility of localized/or selective deposition on patterned substrates. CVD has vast applications in different areas.

There are different types of CVD techniques that are being used today. Examples of CVD techniques include; plasma enhanced CVD (PECVD), metal-organic CVD

(MOCVD), atomic layer deposition (ALD), hot-wire chemical vapor deposition, oxidative chemical vapor deposition (oCVD) etc.

1.3.1 Hot Wire Chemical Vapor Deposition (HWCVD). Hot-wire chemical vapor deposition (HWCVD) is a comparatively new deposition technique that was originally reported in the 1980s[25] and advanced further in the 1990s[26]. Figure 9 displays the number of chemical vapor deposition in the "hot-wire CVD family" publications in a span of 21 years. HWCVD involves the breakdown of a gas precursor through resistively heated filaments.

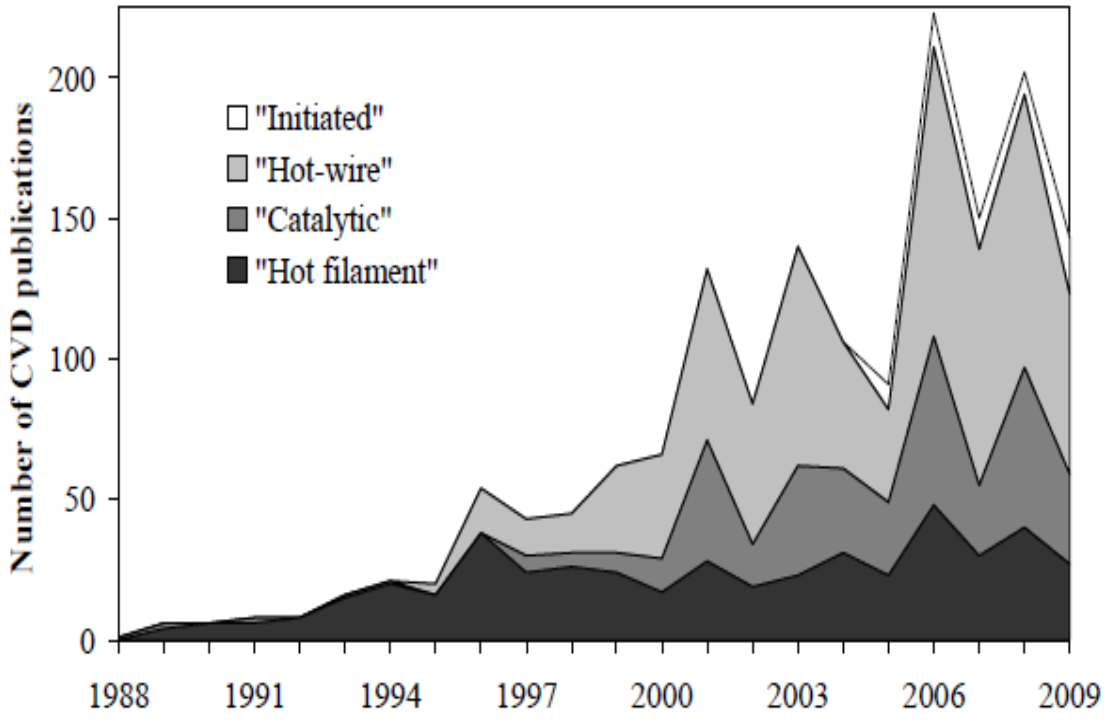

Figure 9: Number of Chemical Vapor Deposition (CVD) publications since the early 1980s in the "hot-wire CVD family" [20].

HWCVD was firstly developed as a substitute to plasma enhanced chemical vapor deposition (PECVD). PECVD utilizes radio-frequency plasma to augment the processes in a chemical vapor deposition (CVD) reactor. However, a disadvantage in PECVD was that if the kinetic energy of the accelerating ions in the plasma is greater that ~20 eV, the substrate surface or the formerly deposited layers could be spoilt. Figure 10 below shows a schematic representation of a HWCVD process of silane (SiH_4) deposited on a substrate.

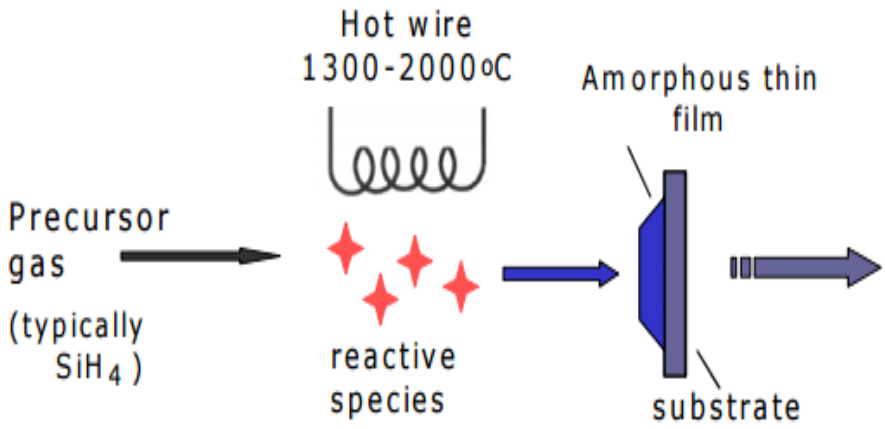

Figure 10: A representation of a hot wire chemical vapor deposition process of silane (SiH_4) gas on a silicon substrate.

1.3.2 Initiated Chemical Vapor Deposition (iCVD). Initiated Chemical Vapor Deposition (iCVD) is an adaptable technique that is used to synthesize conformal and functional polymeric thin films. One of the earliest processes and was originally

demonstrated at the Massachusetts Institute of Technology (MIT) in Professor Karen Gleason's lab in the late 1990's[27]. It is a subfamily of hotwire chemical vapor depositions (HWCVD), and it was originally illustrated for polytetrafluoroethylene (PTFE) thin film deposition with sulfonyl fluoride used as an initiator[28]. The main difference in iCVD and HWCVD technique is that in iCVD, hot filaments are used to break down initiators into free radicals which then gets the process of deposition going, hence the term "initiated".

Past and current iCVD researches have reported the use of resistively-heated array of filaments to thermally decompose initiator inside a vacuum chamber. It has been reported that volatile initiators such as tert-amyl peroxide (TAPO)[29], trimethylamine (TEA)[30], perfluorooctane sulfonyl fluoride (PFOSF)[20], and tert-butyl peroxide (TBPO)[31] thermally dissociate at the surface of the hot filaments or within the hot gas zone. The hot filaments drive the decomposition of the initiators. The surface of the substrate to be cool is actively cooled by circulation of chilled water in the substrate holder to promote adsorption of the species necessary for the growth of the film.

The principle of iCVD works in a three-step process, (a) initiation (b) propagation, and (c) termination. A precursor gas (one or more monomers/co-monomers) and an initiator are metered into a vacuum chamber using mass flow controllers (MFC) or needle valves that control the flow of the gases into a reaction chamber. Inside the chamber is an array of heated filaments and a cooled substrate on which the polymer is deposited. The role of the resistively heated filaments is to create free radical species from the initiator and also to thermally decompose the monomer to generate polymerization species[32]. It has been shown in previous research work that without the

introduction of initiator, thermal decomposition of monomer or contaminants in the reactor yielded species that creates unintended initiation of a polymer chain[24].

In iCVD, polymerization rate and film growth is dependent on the amount of monomer adsorbing on the cooled substrate surface[33]. Keeping substrate surface at low temperatures fosters monomer adsorption which leads to increased rates of film deposition and yields polymer chains of high molecular weight[34]. Typically, a substrate is maintained close to room temperature using backside water cooling[35]. Figure 11 illustrates an iCVD system configuration system and equations showing chemical reactions occurring inside an iCVD reactor during deposition process. The thermal energy from the heated array filaments thermally disassociates the labile bonds of the initiator molecule and as a result generating radical species. The monomer adsorbs onto the cooled substrate underneath the array of filament. Once the initiator radical species are generated, they chemisorb to the adsorbed monomer on the cooled substrate surface initiating a free radical polymerization.

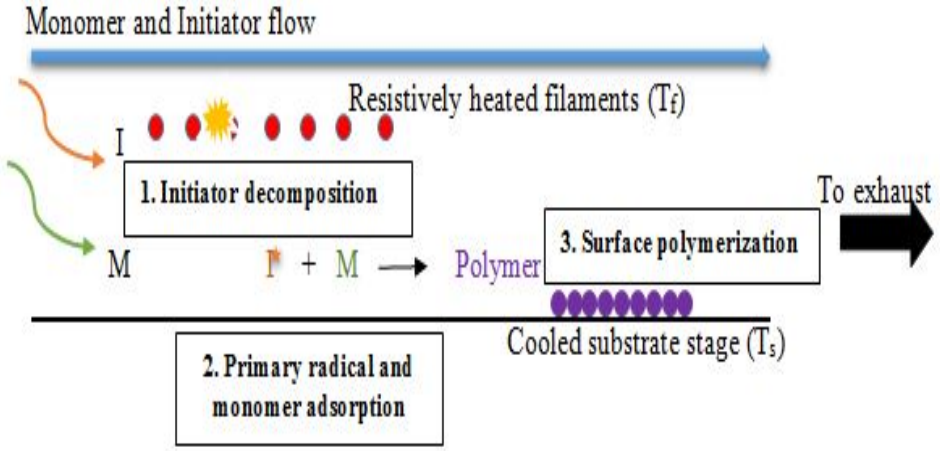

Figure 11: Cross-sectional schematic representation of a typical initiated Chemical Vapor Deposition (iCVD) system configuration[36]. The cross-section shows the mass transfer and reaction during iCVD process. I, initiator; I^*, radical; M, monomer; T_f, filament temperature; T_s, substrate temperature.

The principal iCVD reactions that take place during deposition are shown in equations[37,38] below. Once the initiator is metered into the reactor, it is thermally decomposed through resistively heated filaments to produce free radicals (*I**) (equation1). These free radical species generated from thermal decomposition then impinge onto the surface of the substrate and go through a chemical reaction with the C-C double bond of the active sites of monomer species (*M**) adsorbed on the cooled substrate surface[39]. The monomer species are further added to the active sites of the polymer chain and therefore polymerization propagates[40] (equation 2 and 3). Polymerization process terminates upon the reaction of active sites of a chain with either an active site of another chain or an active site of a free radical[33]. Those radical species that are not integrated into the polymer chain end group during radical termination process (equation 4) could go through a recombination[33] (equation 1, reverse reaction).

$$I_2 \leftrightarrow 2I^* \quad (1)$$

$$I^* + M \rightarrow IM_1^* \quad (2)$$

$$IM_n^* + M \rightarrow IM^*_{n+1} \quad (3)$$

$$IM^*_n + I^* \rightarrow IM_nI \quad (4)$$

CHAPTER 2: DESIGN OF THE iCVD SYSTEM AND EXPERIMENTAL PROCEDURES

2.1 Design of the iCVD Reactor

Atypical CVD can be divided into three broad systems: (1) the gas delivery system, (2) a chemical reaction chamber, (3) and an exhaust system. Usually, the reaction chamber is custom-built to meet specific geometries of the substrates and to incorporate peripherals for process supervision such as real time measurement of the film growth rate using laser interferometry or to acquire real-time understanding of the vapor-phase composition using spectrometers. The precursor delivery system usually differs based on the type of the precursor used that is if the precursor is solid, liquid or gas. Solid precursors are normally melted to form a liquid. Based on the precursor vapor pressure, liquid precursors can be introduced into the reactor chamber using needle valves, flash evaporators, bubbling with a carrier gas, or mass flow controllers (MFCs). The reaction chamber is designed to allow control of process parameters that dictates the reaction kinetics, such substrate temperature, temperature of the heated surface, and total pressure inside the reaction chamber.

A custom built initiated chemical vapor deposition (iCVD) was constructed at the department of Physics, Astronomy, and Material Science at Missouri State University for deposition of polytetrafluoroethylene (PTFE) thin films using perfluoro-1-octanesulfonyl fluoride (PFOSF) as the initiator and hexafluoropropylene oxide (HFPO) as the monomer. The iCVD system was built using a combination of different materials and parts. The system consists of various important sections: reactor chamber, substrate

surface, heated filaments, initiator and monomers jars, mechanical pump, and support equipment as shown in Figure 12 (a). Valves are utilized at different sections of the system and a heating tape exceeding 100˚C is wrapped around the initiator line and the reactor chamber in order to avoid condensation of the initiator inside the walls of the tube and the reactor chamber.

In iCVD system we designed and built in the laboratory, thin film depositions were carried out in a custom-built reactor shown in Figure 12. In Figure 12 (a), the main reactor chamber is shown and all the peripheral devices. Figure 12(b) shows an image of inside the iCVD reaction chamber. Visible inside the reactor chamber are a heat sink, a thermoelectric cooler, an array of filaments, two ceramic blocks attached to a block of copper used to support the filaments and underneath are electrical feedthroughs connected to power supplies outside the reactor chamber.

The reactor chamber is made of stainless steel and is cylindrical in shape with an internal diameter of 20.5 cm and a height of 7.0 cm. A quartz plate, 15.5 cm in diameter is located in the middle of the lid. The transparent quartz will allow future real-time monitoring of the thickness of the growing film as a function of time using a laser interferometer. The exterior wall of the cylindrical reactor was covered with an aluminum foil and a heating tape wrapped around it in order to heat up the reactor. This was done to prevent any condensation of the initiator inside the walls of the reactor. The temperature was monitored and measured using a thermocouple.

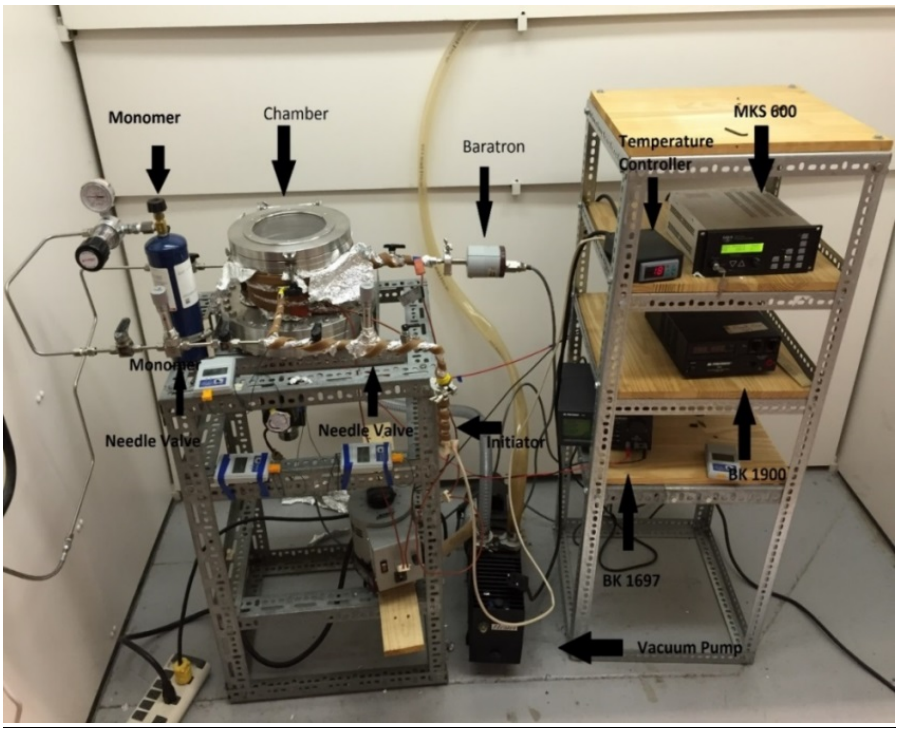

(a)

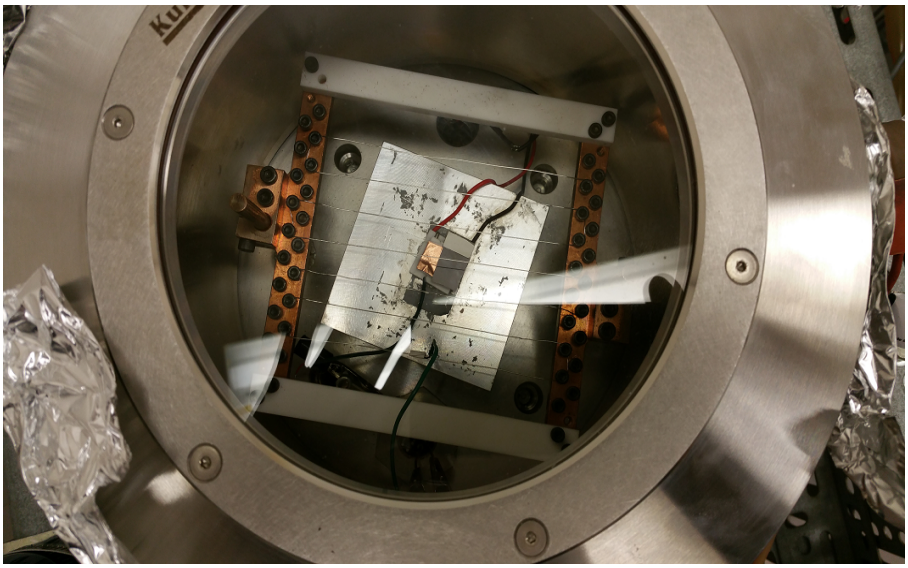

(b)

Figure 12: (a) A real image of the iCVD system setup at Missouri State University with its accessories (b).Top view of the reactor chamber. Inside is a thermoelectric cooler (TEC), electrical feedthroughs, a filament holder and an array of parallel filaments supported two ceramic and copper bars.

Monomer and initiated vapors were metered into the reaction chamber using regulated needle valves (MKS,). Initiator jar was heated to vaporize inside a jar before it is metered into the reaction chamber. The initiator jar and the initiator line are heated up by wrapping a heating tape around them. A digital thermocouple is used to monitor the temperature of the heating tape. Figure 13 shows a schematic representation of an overall overview of the custom iCVD reactor with its peripheral components constructed at Missouri State University.

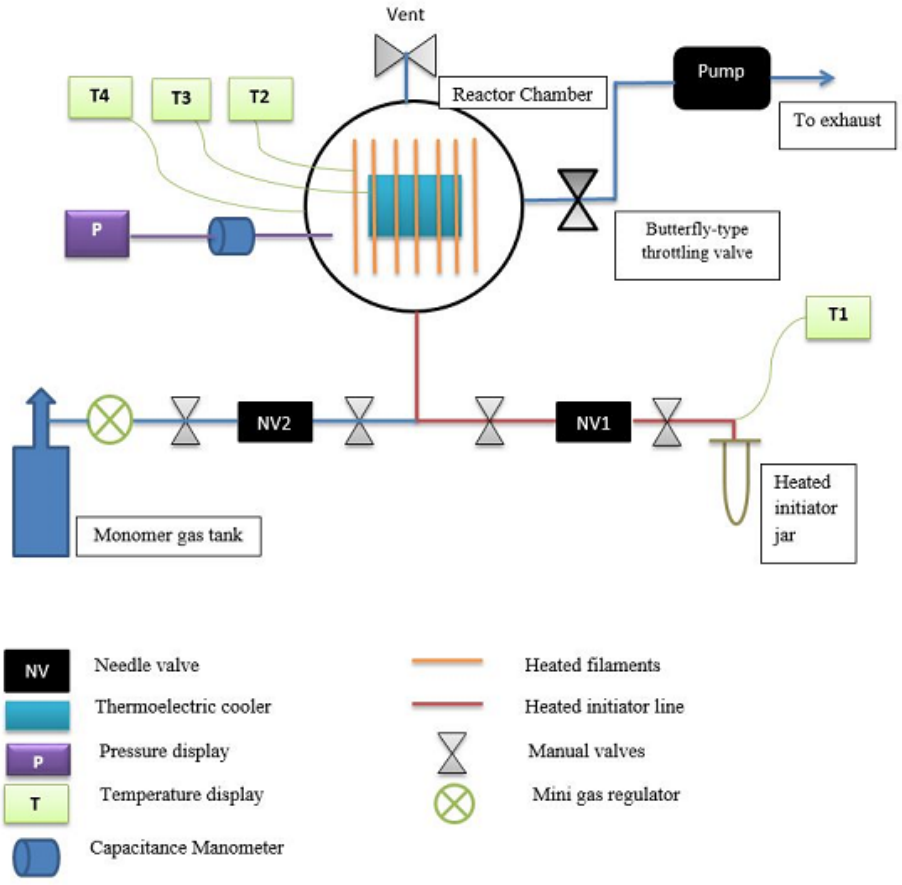

Figure 13: A schematic representation of an overall overview of the iCVD system at Missouri State University.

Nichrome (80% Ni/20% Cr, Omega Engineering) filaments were suspended 1.5 cm above the substrate surface supported with a custom-made ceramic filament holder. There were 8 parallel filaments perpendicular to the direction of flow of gases. The distance between each filament was kept at 1.1 cm. The filaments were resistively heated to a temperature between 250 ºC and 400 ºC, measured using a type-K thermocouple (Omega Engineering) connected directly to the outermost filament. A dc power supply (1697 BK Precision) was used to heat the filaments. A thermocouple probe connected to the outermost filament was connected to a thermocouple outside the reactor through electrical feedthroughs. The electrical feedthroughs are connected to the thermoelectric cooler (TEC, Custom Electric) at the center of the rector to maintain the substrate temperature at a desired temperature, typically at room temperature.

Thermoelectric cooler was securely placed on top of an aluminum block mounted to the base of the reactor. A working principle of a TEC is quite simple. TEC is a semiconductor element that enables cooling, heating and temperature control to be freely conducted with a direct current. By applying a direct current through a TEC module, a temperature difference between the sides of the module occurs. The Low temperature side has an endothermic effect while the higher temperature has an exothermic effect – thus heat is transferred from low temperature to high temperature region. Figure 14 below shows a typical schematic diagram of a characteristic TEC.

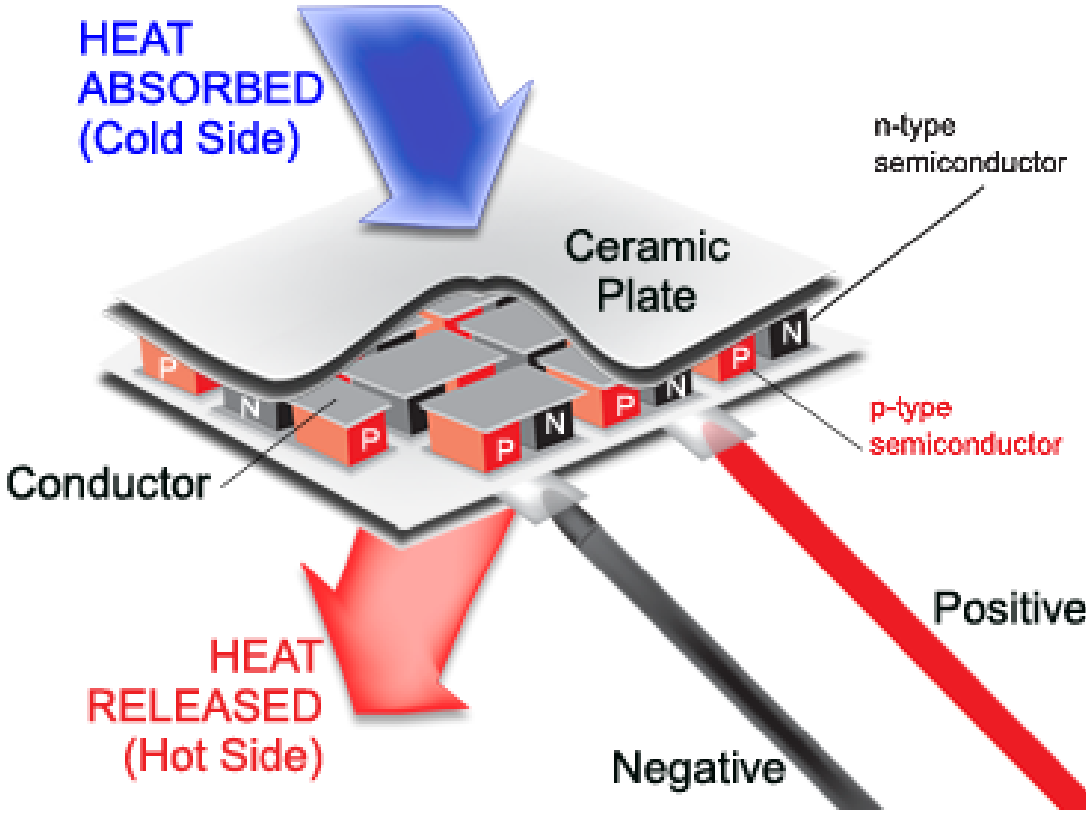

Figure 14: Schematic representation of a typically Thermoelectric Cooler (TEC) [41].

2.2 Description of Chemicals Used and Experimental Procedure

2.2.1 Materials Used. Hexafluoropropylene oxide (HFPO) monomer with 98% % purity was purchased from Sigma-Aldrich and used as it was received without further removal of inhibitor or purification. The radical initiator, perfluoro-1-octanesulfonyl fluoride, with 95% purity, was purchased from Sigma-Aldrich and was used as received.

2.2.2 iCVD Deposition Parameters. The main iCVD parameters that were controlled in this research were reactor pressure, filament temperature, substrate temperature, and initiator temperature, filament to substrate distance, reactor wall temperature, and deposition time. Filament temperature between 300 – 350˚C was

applied on all the samples. The reactor pressure was monitored using Baratron Manometer capacitance (MKS). The test tube holding the liquid initiator heated up 100˚ C ± 5 ˚C in order to vaporize the liquid initiator in the inside the jar. Table 1 shows typical process conditions that were used in the deposition of the iCVD PTFE thin films using the custom built reactor at Missouri State University.

Temperature of the substrate inside the reactor chamber was cooled and maintained using a thermoelectric cooler (TEC). The deposition was done between 3 minutes and 25 minutes. This was done to be able to determine the rate of deposition. For all the samples, a constant filament to substrate distance of 10 – 15 mm was maintained. Before deposition was done, the reactor was pumped down to its base pressure of between 25 – 40 mTorr using a mechanical roughing pump (Alcatel).

Table 1. Typical process parameters and conditions used in this research for initiated chemical vapor deposition (iCVD) of as-deposited PTFE thin films using perfluoro-1-octanesulfonly fluoride (PFOSF) as the initiator.

Sample IDs	Parameters	Conditions
All samples	Reactor Pressure	1.1 − 3.5 Torr
	Filament Temperature	300 − 370 ˚C
	Filament Type	Nichrome (80% Ni, 20% Cr)
	Substrate to filament distance	10 – 15 mm
	Substrate Temperature	10 – 32 ˚C

2.2.3 Synthesis of PTFE Thin Films. iCVD polytetrafluoroethylene (PTFE) thin films were deposited on silicon wafers carefully placed inside a reactor. A custom-built iCVD vacuum reactor with a base pressure of between 25 and 35 mTorr was used to grow the thin films. The diameter of the cylindrical reaction chamber is 25.4 cm and a height of 7 cm. The top of the reaction chamber has a thick transparent quartz lid with a diameter of 15 cm. The transparent quartz lid was added in order to be utilized in the future to monitor film growth and thickness of the film in real time using a laser interferometer. The reactor chamber pressure was measured using a Baratron capacitance manometer (MKS instruments) and adjusted using a downstream throttle valve. The vacuum of the reaction chamber was obtained by means of a mechanical roughing pump (Alcatel). Inside the reaction chamber was an array of 8 parallel nichrome filaments (80:20 Ni/Cr, Omega Engineering) resistively heated using a dc power supply (1697 BK Precision) in a steady current mode. The surface temperature of the substrate was maintained using a thermoelectric cooler. The temperature of the reactor wall, filaments, and substrate were monitored with type K thermocouples (Omega Engineering).

The PFOSF initiator was heated in a small jar to 110 ˚C ± 5 ˚C and the stainless steel line connecting initiator jar and the reactor chamber was heated to a temperature of 95 ˚C ± 5 ˚C. HFPO monomer was already in gaseous form and needed no heating. The reactor wall was heated to a temperature of 78 ˚C to prevent any condensation of the reactants and gaseous products inside the reaction chamber. Monomer and initiator were metered into the reaction chamber using two needle valves (Swagelok). In all deposition runs, the range of substrate temperature was maintained between 15 and 31 ˚C, the range of filament temperature was maintained between 300 ˚C and 400 ˚C. The distance

between the nichrome (80% Ni, 20% Cr) filaments and the surface of silicon wafer was kept at 1.5 cm. Silicon wafers were sonicated in isopropyl alcohol for 5 minutes and dried in air before being placed on the surface of a thermoelectric cooler (TEC) inside the reaction chamber. A thermal sheet was placed between the wafer and the TEC to provide good heat conduction and stability of the wafer when the pump is running.

Hexafluoropropylene oxide was thermally decomposed inside the iCVD reaction chamber to yield difluorocarbene (CF_2) molecules and trifluoroacetyl fluoride ($CF_3C(=O)F$), a relatively stable by-product[42]. Difluorocarbene molecules then join together to produce a long chain of PTFE ($-(CF_2)n-$)[43] deposited on the surface of cooled substrate as shown schematically in Figure 15 below.

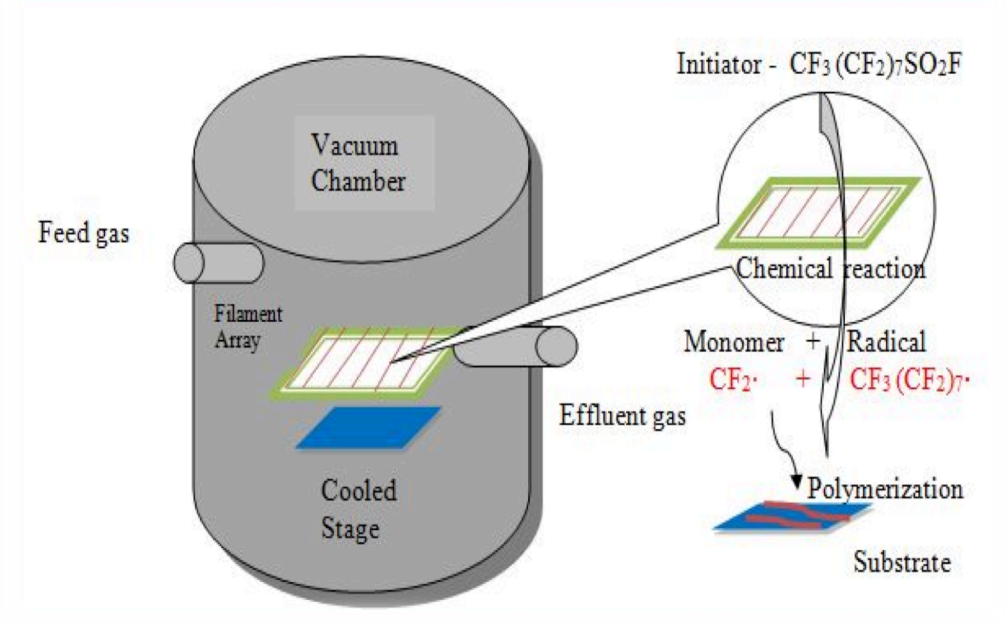

Figure 15: A schematic representation at Missouri State University of iCVD process for growing PFTE thin film using perfluoro-1-octanesulfonyl fluoride (PFOSF) as the initiator and hexafluoropropylene oxide (HFPO) as a monomer. Shown is a gas inlet from the side of the reaction chamber, thermal decomposition on the square filament array (insert), and deposition onto a substrate sitting on a cooled surface.

CHAPTER 3: BASIC PRINCIPLE AND THEORY OF THE CHARACTERIZATION TECHNIQUES USED

Several characterization techniques have been successful in identifying the polytetrafluoroethylene (PTFE) sample. Other properties such as the constituting elements of the sample could be traced as well as the existence of defects within its lattice structure. In the course of this research work, X-ray diffractometer and Raman spectroscopy did not reveal any feature peaks and no information could be acquired from their corresponding data. This could possibly be due to the amorphous nature and thickness of the thin film layer. Hence, other techniques such as scanning electron microscope (SEM), Fourier transform infra-red (FTIR) and atomic force microscopy (AFM) were employed to give more detailed data. Below are detailed descriptions of all the experimental characterization techniques used for the research work.

3.1. Fourier Transform Infrared (FTIR) Spectroscopy

The first infra-red (IR) spectrometer tool was developed as far back as 1950's. It used a sodium chloride prism for optical splitting of infra-red beams. The use of this splitter comes with strict sample's water content and particles size. Later developments led to the production of the second generation infra-red spectrometer in the 1960's, known as the dispersive IR spectrometer. It was an improvement in the previous equipment. Gratings were used as the monochromater[44]. Some challenges encountered while using the dispersive IR spectrometer included low sensitivity, low scan speed and poor accuracy in wavelength. The most recent Fourier transform infra-red (FTIR)

spectrometer is a vast improvement in terms of simultaneously passing multiple monochromatic light of different frequencies unto the sample, thereby improving the speed in data collection. Fourier transformation is a mathematical method derived by French scientist, Jean Baptist Joseph Fourier which has been utilized to transform cosine wave of the interferogram to an interpretable spectrum of transmittance and wave number cm^{-1}.

The basic working principle of FTIR is very different from that of dispersive IR spectrometer. The components of FTIR include the infrared beam source, an interferometer consisting of a beam splitter, a stationary and movable mirror; it also includes a sample compartment, detector, amplifier, A/D convertor and a computer. The stationary and movable mirrors are placed perpendicular to each other, while the Fourier transformation is done inside the computer.

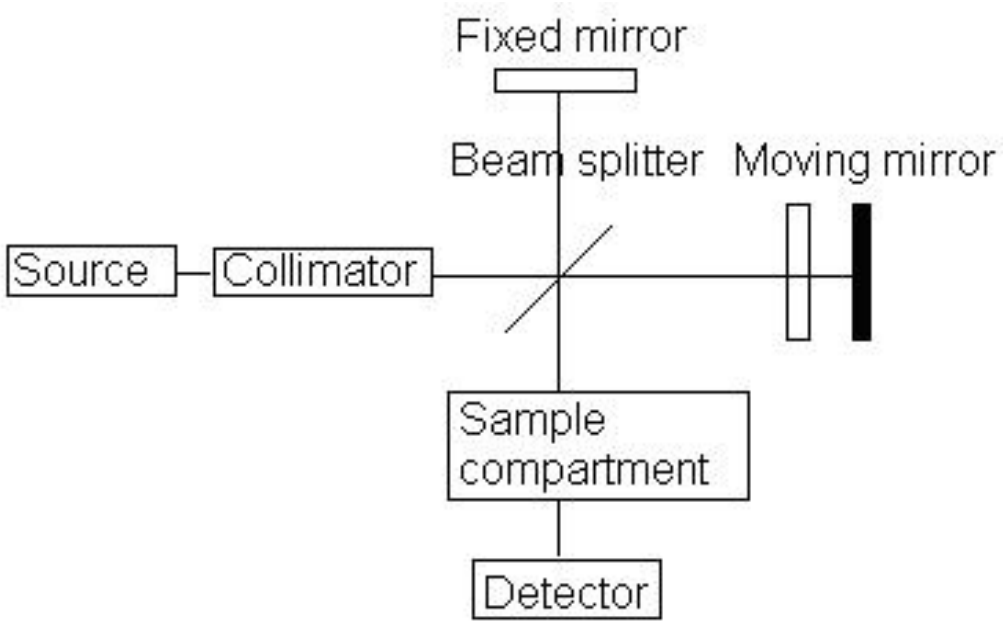

Figure 16: Schematic diagram of an FTIR spectrometer**.**

The infra-red beams are passed through the collimator unto the beam splitter which replaces the grating used in dispersive IR spectrometer. The beam splitter is designed to split the beam into half; 50% of the spectrum is reflected to the stationary mirror while the other 50% is transmitted to the rotating mirror which is perpendicular to the first mirror and of equal distance from the beam splitter, a term known as zero path difference (ZPD). The beams are then reflected back to recombine at the beam splitter. These recombined infrared beams consist of multiple monochromatic beams of varied frequencies. Since the movable mirror is not in a fixed position, it generates three categories of reflected beams recombining with those reflected from the stationary mirror[29,45].

When the movable mirror rotates as the transmitted light travels toward it, this causes the light beam to travel farther distance than those refracted toward the fixed mirror. The additional distance travelled by this transmitted light is known as the optical path difference (δ), which is equal to 2 times the displacement of the movable mirror from the ZPD (Δ).

$$\delta = 2\Delta \qquad (1)$$

When the optical path difference (OPD) is an integral multiple of the wavelength of the initial incident infrared light, then a constructive interference occurs at the beam splitter with recombining beam from both mirrors having their respective crests and trough overlapping.

$$\delta = n\lambda \qquad (2)$$

When it happens that the OPD is an integral multiple of half wavelength of the initial source light then you have a destructive interference and the equation of the optical path difference is as shown below.

$$\delta = (n + \frac{1}{2})\,\lambda \qquad (3)$$

Hence the crest of the beam from the fixed mirror overlaps with the trough of the movable mirror beam. Finally, when OPD is neither an n nor $(n + \frac{1}{2})$ -fold of wavelength in both extreme cases discussed above the interference is between destructive and constructive interference.

Since the Michelson interferometer is the core component of FTIR which includes both mirrors and the beam splitter, the recombined beams are directed to the sample compartment as shown in the schematic diagram of FTIR in figure 1. Figure 17 depicts a schematic representation of Michelson's interferometer.

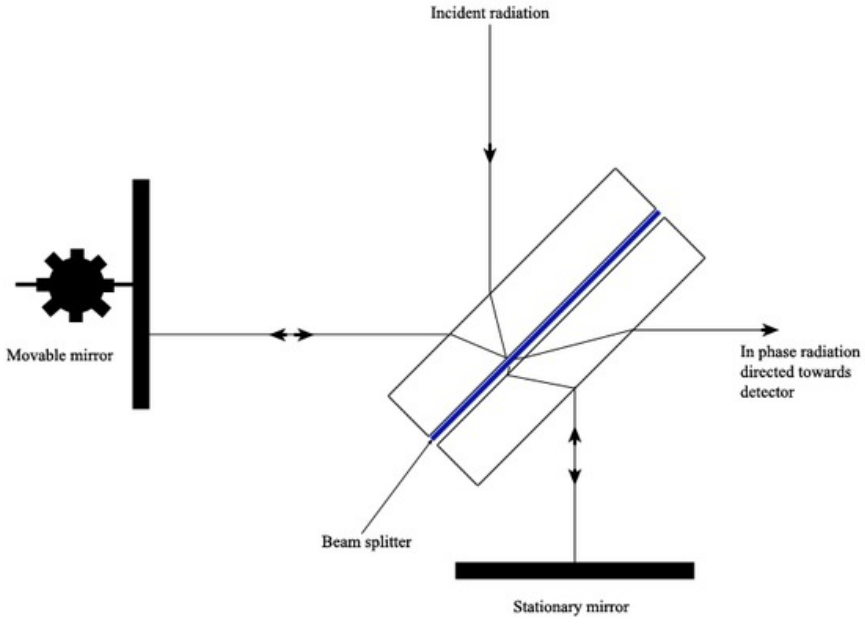

Figure 17: Michelson interferometer schematic diagram.

The beams incident on the sample are either reflected or transmitted and collected at the detector as beam signals known as interferogram. This is a cosine wave which cannot be interpreted by analyst. Therefore, it is necessary to convert this interferogram to a plot of intensity at each individual light frequency using Fourier transformation. Figure 18 shows the process from which beam signals are converted from interferogram FTIR spectra.

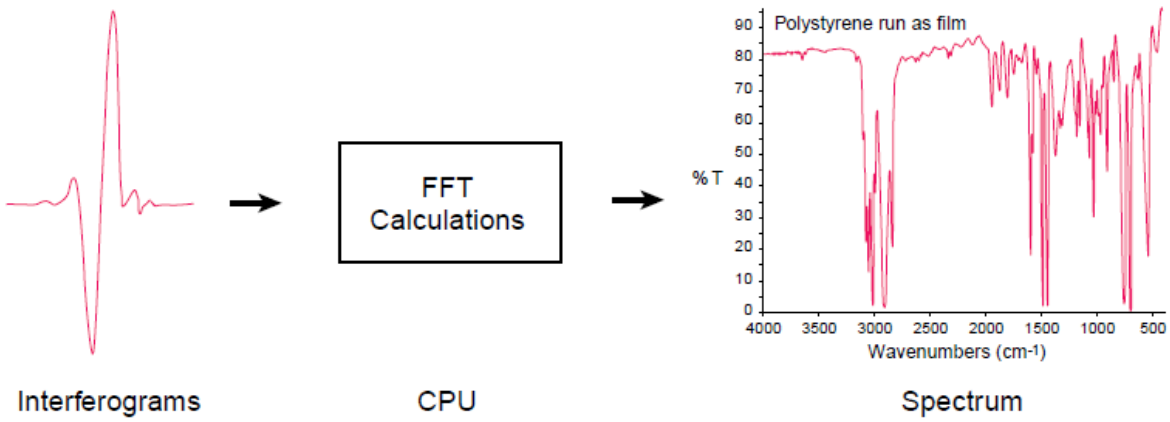

Figure 18: Conversion of interferogram to transmission plot

3.2. Scanning Electron Microscopy (SEM)

The strength of this equipment in analyzing a sample cannot be over emphasized. Scanning electron microscope (SEM) was developed as far back as 1935, since then its popularity amongst scientists has grown so much with an estimated 50,000 SEM equipment filling laboratories across the globe. Figure 19 shows SEM setup that we used to analysis as-deposited iCVD PTFE thin films at Jordan Valley Innovation Center in (JVIC) Springfield, MO. The advantage of SEM over regular optical microscope is its

increased magnification power of about 300,000 times the size of an object. Also images created by SEM can be seen in 3D which makes it even more real to the human eye. The human eye can distinguish particles separated by a distance of about 0.2 mm under bright light. This is called the resolving power resolution of the eye. With scanning electron microscope, closer particles could be viewed as separate due to the high resolution.

Figure 19: Image of Scanning Electron Microscope (SEM) setup.

Breakthrough in SEM has also been recorded in forensics for crime scenes which is why the importance of its application is very broad[46]. Unlike regular optical microscope, the SEM requires special sample treatment before viewing under the microscope. All samples studied using SEM have to have a conducting surface which is why there is no special treatment for samples with conducting surface. However, for non-metals and biological sample specimens, the surface has to be coated with thin film of

metallic agent such as gold or platinum using sputter coating technique. The non-metal sample is placed inside the sputter chamber in the presence of argon gas. Electric field is applied which ionizes the gas creating positive argon ions. These Ar^+ ions are then attracted to the negatively charged gold foil knocking atoms off it. The gold atoms fall on the surface of the non-metal sample coating it in the process.

Also since the experiment is usually performed under low vacuum pressure most samples are always dried up before analysis to prevent the formation of water vapor in the vacuum chamber thereby distorting the image generated. The reason for using samples with good conducting surface is for proper grounding of the sample in order to prevent charges from storing up at the surface of the sample. This is what will occur if the sample is non-metallic without sputter coated surface.

SEM acquires images from a particular sample by using secondary electrons, back scattered electron and characteristic X-rays falling on the detectors in the chamber. The principle of a typical SEM is quite straight forward. Electrons are accelerated from an electron gun. The electron guns used are either thermionic or field emission. The thermionic gun uses thermal energy which generates electrons from a tungsten filament while field emission gun uses electric field. SEM uses electromagnetic lenses to focus the electron rather than glass lenses used in optical microscope. There is a winding of scanning coils along the path of motion of the electron as it travels inside the chamber. The scanning coil is used to control its path which helps in focusing the beam on a particular region on the surface of the sample. As soon as the beam of electrons hits the sample surface it interacts with the electrons of the sample surface and inside the

structure of the sample. The interactions that occur are of three types. These interactions are shown in Figure 20.

The first one is primary backscattered electrons (BSE) which are reflected off the surface structure of the sample by elastic scattering. When collected at the detector, its signals are used to understand the distribution of different elements in the sample because the intensity of BSE is directly related to the atomic number of the sample atom interacting with it.

The characteristic x-ray is another type of emission that occurs due to the interaction between the accelerated electron from the electron gun and the electrons in the innermost shell of the atoms of the sample. This interaction causes the inner shell electrons to be removed and replaced by higher energy electron resulting in the release of energy in a form of x-ray emission. The composition and measurement of the abundance of various elements in the sample are identified with the help of the characteristic x-rays detected at the x-ray detector.

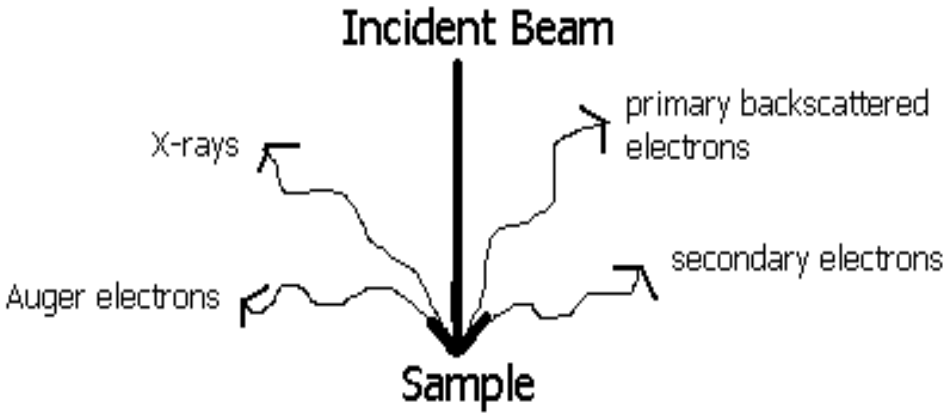

Figure 20: Interaction between accelerated electrons and the sample.

The secondary electrons are generated from knocking of the outer electrons from the atoms of the sample surface. They are collected at the SE detector and are used to generate the image of the surface topography and structure of the sample. The components of a scanning electron microscope device can be broken down into the following major components; electron gun, electron beam, first condenser lens, second condenser lens, deflection coils, x-ray detector , and backscatter electron detector. Figure 21 below shows a schematic diagram of scanning electron microscope internal components.

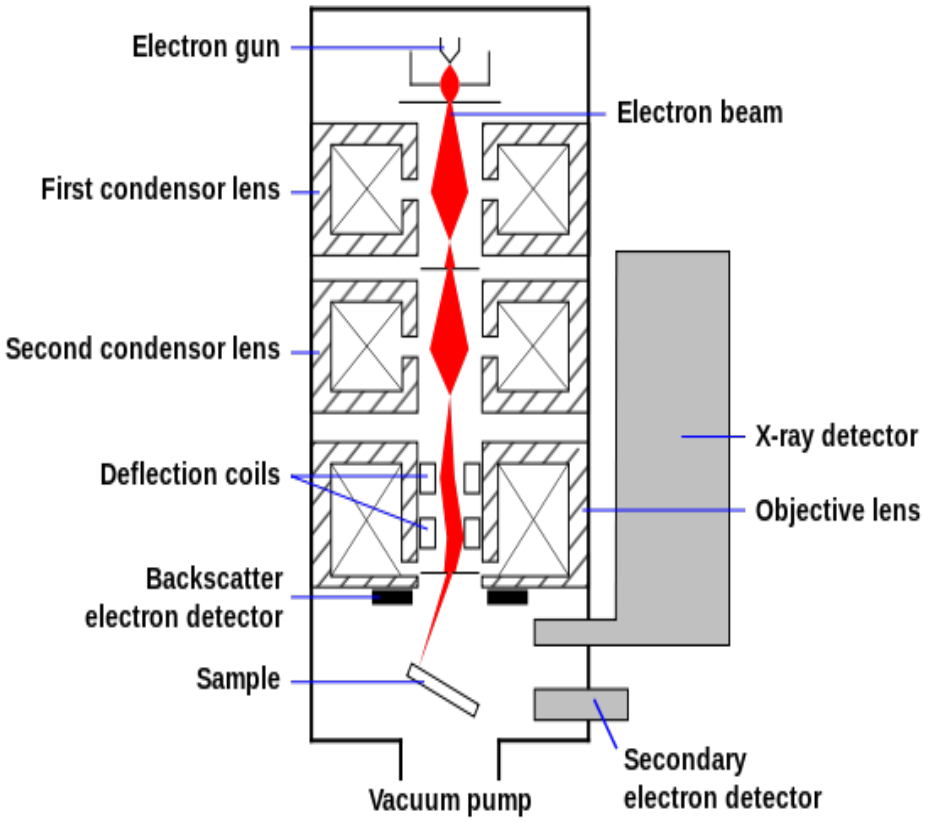

Figure 21: A schematic diagram of a SEM interior [47].

The electron gun is the source of electrons that are accelerated toward the surface of the sample in the sample chamber. This electron gun could either be thermionic or field emission and serves as the cathode. The electron beam is then passed through the two sets of condenser lenses which focuses the beam. There is a scanning deflection coil along its path of motion through a final lens; this controls the movement of the electron beam using fluctuating voltage from magnetic field. The deflected electron beams are directed toward the surface structure of the sample thereby interacting with the electrons from the atoms of the sample. Three dedicated detectors for each of the inelastic secondary electrons, elastic backscattered electrons and characteristic X-rays are positioned to collect these particles, converting them to signals that could create 3D images of the sample under study. A vacuum pump is attached to the chamber in order to achieve high vacuum pressure inside the chamber.

For good results and safety measures, it is important that the SEM is properly closed to avoid exposure to x-rays. Also, it is important that experiments be performed in a non-vibrating environment due to the high sensitivity of SEM to vibrations. A sample placed inside the chamber should be rid of water molecules, because at low pressure this water content vaporizes causing obstruction to the path of the traveling electrons and even leading to collision between the electron beams and vapor.

Control of image resolution formed and analysis of the composition elements of the samples are manipulated using EDX on a computer. EDX is a tool that works in conjunction with SEM. It is used to control the energy of the electron beams, resolution, area of scan, vacuum pump and venting of the chambers and many more functions

3.3 X-ray Photoelectron Spectroscopy (XPS)

X-ray Photoelectron Spectroscopy (XPS) also termed as Electron Spectroscopy for Chemical Analysis (ESCA) is a commonly used technique for investigation of chemical composition of surfaces. Other information that can be obtained from XPS includes identification of elements near the surface and surface composition, local chemical environment, the valence electronic structure, and thin film morphology.

A heated filament (cathode) emits electrons which are then accelerated toward the anode (which is cooled with water) over a potential of the order of 5-20 kV. As the electrons bombard the anode, holes are created in the inner levels of the anode which are radioactively filled by electron transitions from higher levels. Figure 22 depicts a schematic representation of a photoelectric process. XPS spectra lines are identifiable by the shells from which the electrons are ejected from.

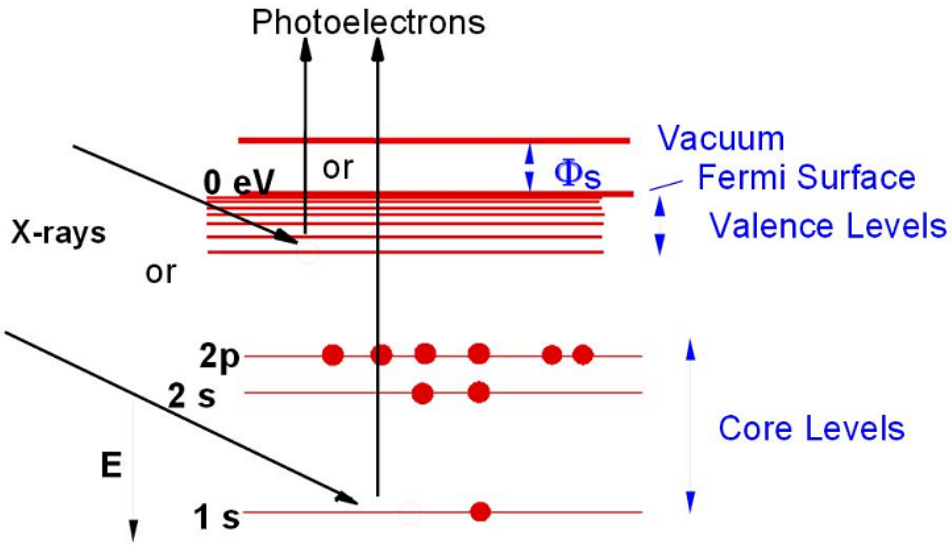

Figure 22: Diagram of a photoelectric process. XPS spectral lines are identified by the shell from which the electron is ejected from i.e. 1s, 2s, 2p, etc.

The correlation dictating the interaction of a photon with the core level is given by;

$$\mathbf{BE = h\nu - KE - \Phi_{spec}}$$

Whereby: BE is the binding energy of the atomic orbital of which the electron emanates

$\mathbf{h\nu}$ is the distinctive energy of an x-ray photon

KE is the kinetic energy of an ejected photoelectron from the sample

$\mathbf{\Phi_{spec}}$ is the spectrometer work function

3.4 Atomic Force Microscopy (AFM)

This is a type of scanning probe microscopy (SPM) developed by Binnig and Quate in 1986[48]. Figure 23 is a setup of an Atomic Force Microscope found at Jordan Valley Innovation Center (JVIC) in Springfield, MO. This AFM equipment was used to characterize the samples. Unlike the scanning tunneling microscope that uses electron probe, atomic force microscopy makes use of a probing tip and a cantilever to measure the surface topography of a thin film sample.

Atomic force microscopy can be used to measure sample heights, surface frictions and topographies as compared to scanning tunneling microscopy. Another advantage of atomic force microscopy over scanning tunneling microscopy is that it can be used to analyze electrically non-conducting sample surface. It can be used in air and water atmosphere. The probe tip is very sharp with a 3-6 μm length with a tip radius of between 15-40 nm. This makes for a better resolution of the image formed than a thicker tip radius. The lateral resolution is usually low (~30 nm) while the vertical resolution is typically high (0.1 nm)[49].

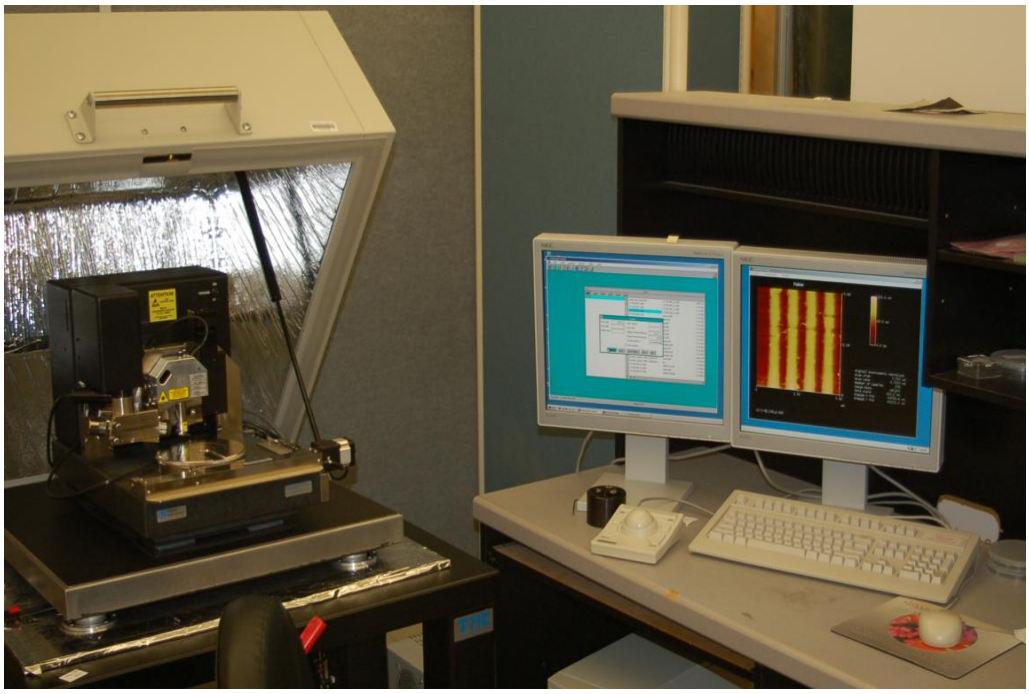

Figure 23: Atomic Force Microscope (AFM) setup.

As mentioned earlier atomic force microscopy (AFM) consists of a probe tip attached to a piezo cantilever; other components includes a laser diode, a position sensitive detector and a feedback loop. The interaction force acquired during measurement is converted to signals used in creating a corresponding image for the surface and height of the sample. Images formed from AFM are usually in three dimensions along the x, y and z axes. Figure 24 shows central components of an AFM equipment.

The principle of atomic force microscopy is based on the measurement of the force between the probe tip and sample surface. It also uses both the forces of attraction and deflection. All through the measurement the force between the probe and sample is kept constant irrespective of the surface topography. This can be achieved through a feedback loop, which constantly adjusts the interacting force. The photodiode is a laser

source which directs the beam of light on the back of the cantilever. The reflected light is collected by the positioned sensitive detector. The detector uses this information for creating an image.

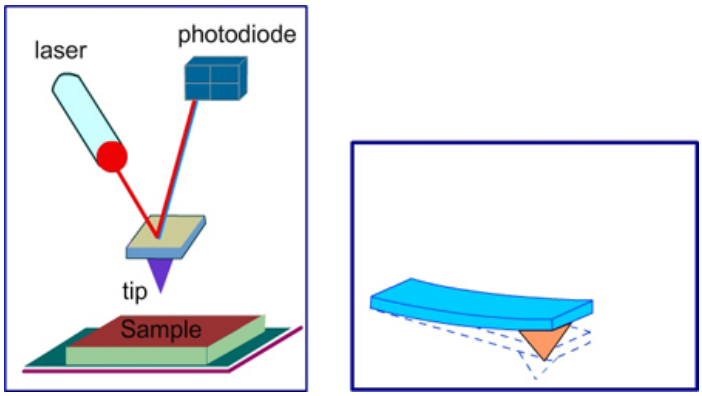

(a) (b)

Figure 24: Diagram of crucial AFM components. (a) shows a representation of the tip; it contains a probe straddled on a cantilever, and in (b) the cantilever easily bends even with a slight force on the tip.

The photo sensitive detector is divided into four segments: this tracks the position of the laser spot on the detector and thus measuring the angular deflections of the cantilever. The most common type of probing mode is the contact mode in which the tip is in constant contact with the sample surface. The flexible cantilever bends towards the surface of the sample as the probing tip approaches from a distance due to attraction force. When the tip scans through the surface it repels and bends away from the surface once it encounters a height thereby maintaining the force of interaction. This is due to a reduced tip-sample distance leading to an overlap in the electronic orbitals of the atomic distances. This causes a repulsive force of interaction as shown in Figure 25.

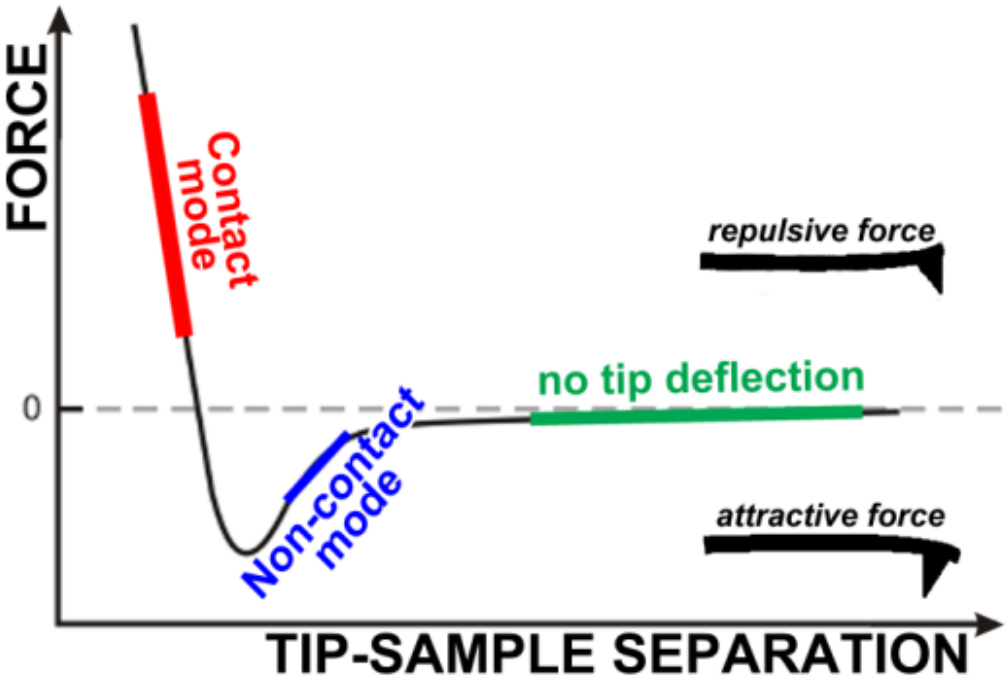

Figure 25: A plot of force as a function of tip-sample separation.

The other type of AFM is the dynamic force mode which includes (tapping and non-contact mode). For the case of tapping mode, the probe keeps oscillating in the repulsive region at a resonance frequency as it rasters through the surface of the sample. Amplitude of oscillation is kept constant at about 10 - 50 nm. In the like manner, the laser source passes light beam reflected by the back of the cantilever. In the tapping mode challenges such as the probe scratching the surface of soft samples can be prevented. Tapping provides higher resolution with reduced sample damage. It has the advantage over contact mode because it measures surface topography of fragile biological samples. Image formed is due to its amplitude signals as the surface rises and falls across the sample. This mode is known as an intermittent between the contact and the non-contact mode.

Another important mode is the non-contact. In this case, the cantilever oscillates at much lower amplitude of (< 5 nm). Hence, the interaction between the tip and sample is that of attractive Van der Waal force due to the relatively larger separation between the tip and sample compared to atoms of the sample. Non-contact mode becomes useful in fluid samples and water droplets. Figure 26 shows a difference between a contact and non-contact mode as the cantilever moves through and over a water molecule respectively.

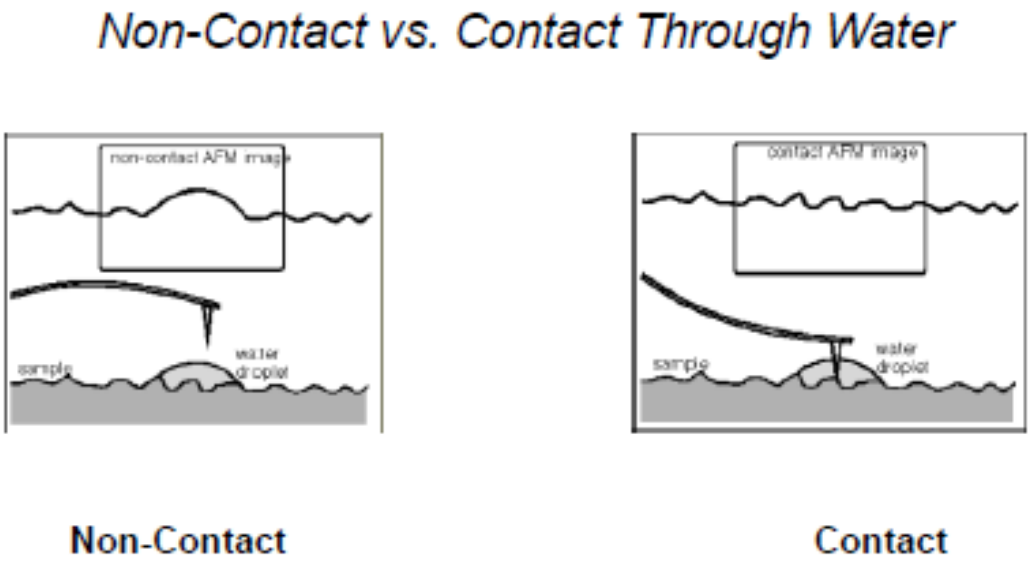

Figure 26: A comparison between a non-contact and contact mode over and through a water droplet.

CHAPTER 4: RESULTS AND DISCUSSIONS

This chapter gives analysis of samples deposited using the custom-built initiated Chemical Vapor Deposition (iCVD) technique. In addition, this section will use the results obtained to support the goal of this research which was to successfully deposit polytetrafluoroethylene (PTFE) thin films using a custom-built initiated Chemical Vapor Deposition (iCVD) reactor with perfluo-1-octanesulfonyl fluoride (PFOSF) and hexafluoropropylene oxide (HFPO) being the initiator and the monomer, respectively. This section presents analysis of data collected from Fourier Transform Infrared (FTIR) spectrometer, X-ray photoelectron (XPS) spectrometer, Scanning Electron Microscope (SEM), EDS, and Atomic Force Microscope for the samples deposited using a custom-built iCVD reactor. Table 2 summarizes the different parameters that were used to grown various iCVD PTFE samples.

Table 2: List of iCVD PTFE thin films samples grown a different parameters.

Sample ID	Filament Temp. (˚C)	Substrate Type	Substrate Temp. (˚C)	Pressure (Torr)	Deposition time (mins)
112014_PTFE	316 – 321	Silicon	29.5 ± 1.5	3.35 ± 0.15	25
120414_PTFE	310 – 314	Silicon/Glass	16.0 ±1.0	3.30 ± 0.20	10
011315_PTFE	355 – 360	Silicon	10.0 ± 2.0	1.05 ± 0.01	5
020915_PTFE	301 – 305	Silicon	29.5 ± 1.5	1.14 ± 0.01	4
020515_PTFE	292 – 300	Silicon	9.0 ± 3.0	1.50 ± 0.30	3

4.1. Fourier Infrared Transform (FTIR) analysis of iCVD PTFE Thin Films

Fourier-transform infrared (FTIR) spectra of iCVD PTFE thin films were obtained using Bruker Vertex 70 FTIR with Raman accessory, Perkin Elmer 1750 operated with KBr detector. FTIR was used to obtain information about chemical composition of as-deposited iCVD PTFE samples though the analysis of molecular vibrational modes. iCVD samples to be analyzed were irradiated with a light beam, therefore, exciting vibrational states into a higher energy level. FTIR spectra was collected over a range of 4000 – 400 cm^{-1} at a resolution of 4 cm^{-1}, averaged over 500 scans and baseline corrected. FTIR spectroscopy was used to substantiate the chemical structure of iCVD deposited thin films.

Our FTIR absorption peak assignment was based on literature. These absorption band assignments are summarized in Table 3 which shows band assignment of linear CF_2 vibrational modes that are spectroscopically analogous of bulk PTFE. Figure 27(a) shows an FTIR spectrum of as-deposited iCVD PTFE thin film two. We observe two prominent absorption peaks at 1213 and 1155 cm^{-1}. These two absorption bands are attributable to CF_2 asymmetric and symmetric stretching modes respectively[50,51,52] This doublet is spectroscopically distinctive of bulk PTFE as shown in Figure 27(b). The absorption peak observed in Figure 27(a) in the region between 500 and 700 cm^{-1} is assigned to -CF_2- wagging of the iCVD PTFE molecule[53]. We note that the intensity of these absorption peeks are low, and as a result limit the detection of –CF_2- wagging in this region. Naturally, the peaks in this region have weaker absorption[54]. Additional FTIR spectra of as deposited iCVD PTFE thin films have shown in the appendix.

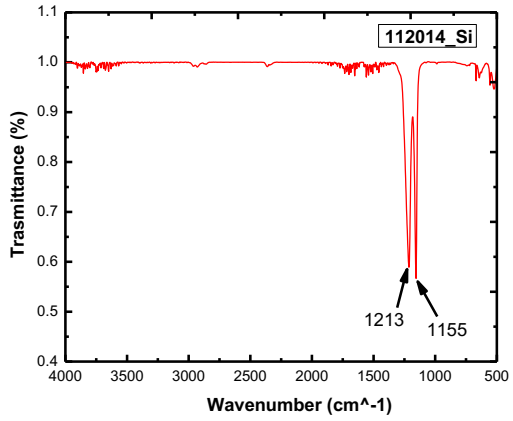

(a)

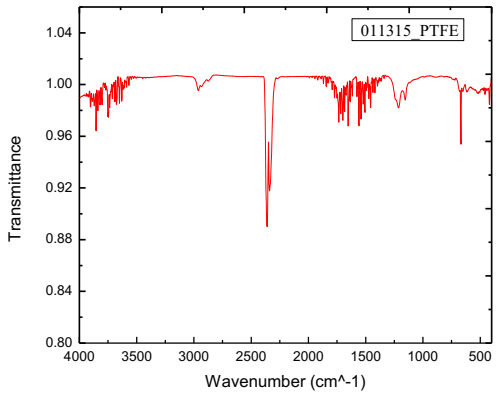

(b)

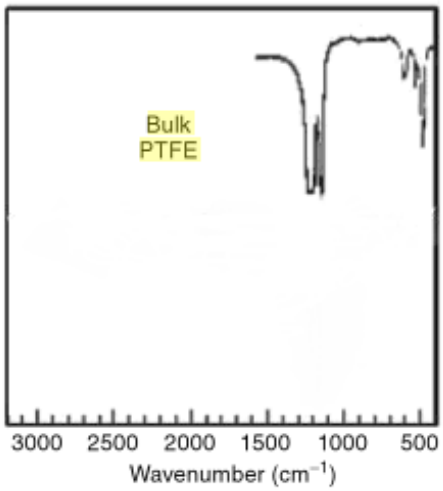

(c)

Figure 27: FTIR spectra of as deposited iCVD PTFE thin films (a) sample 112014, and (b) sample 011315. All the samples were deposited at different deposition conditions. (c) FTIR spectrum of bulk PTFE.

Table 3: Absorption band assignment for FTIR spectra

Assignment	Wavenumber (cm^{-1})	Reference
CF_2 symmetric stretching	1155	55, 56
CF_2 asymmetric stretching	1215	34, 35
CF_2 deformation	555	34,35
CF_2 wagging	641/629	34, 35
CF_2 rocking	513/530	34, 35
C=O/COO in CF_xCOO^-	1708	57
OH	3523	58

4.2. X-ray Photoelectron Spectroscopy (XPS) Analysis of iCVD PTFE thin films

Another vastly utilized characterization technique is X-ray photoelectron spectroscopy (XPS). XPS has been used for decades as a way for material characterization. It is a reliable method for determining the types of functional groups on the surface of a polymer. In this research, XPS was done using Thermo Fisher Alpha 110 equipped with an XR5 monochromatic X-ray source. One of the issues in polymer analysis is surface charge build up as a result of surface electron loss through X-ray radiation. To counter this problem in our XPS analysis, 25 μA of low energy electron beam (-4V) was applied using Thermo Fisher FG01 electron flood gun to avoid charge build up on the surface of the sample. From the XPS spectra we obtained, we can infer that the major elements in the iCVD PTFE thin film are carbon (C) and fluorine (F) which we expected.

From iCVD PTFE survey scan in Figure 28(a), we observe that the position of C_1 (292 eV) and F_1 (685eV) peaks is similar to that of Figure 29, an XPS survey scan of bulk PTFE. This confirms that the PTFE thin film was successfully deposited using a custom built initiated Chemical Vapor Deposition (iCVD) reactor. The prevalence of the $–CF_2–$ bonding environment in the iCVD deposited thin films was verified by X-ray Photoelectron spectroscopy (XPS). Figure 28 shows XPS spectra for sample 120414 deposited on both silicon and glass substrates at the same deposition parameters.

The most prominent peak at 292.1 eV resembles the CF_2 groups and characterizes 90% background content of polymers[59]. This confirms that PTFE is present on the surface of the silicon substrate, and overall the chemical structure of the thin film is analogous to that of bulk PTFE. By comparing XPS survey scan of iCVD PTFE in Figure 28 and that of bulk PTFE in Figure 29, we observe that the two are characteristically identical.

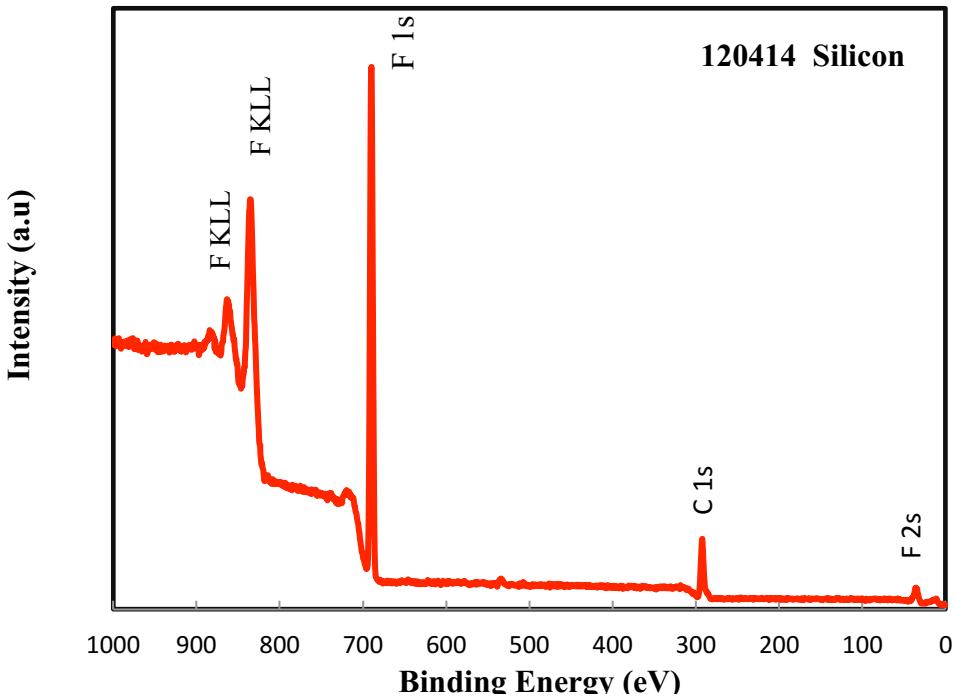

(a)

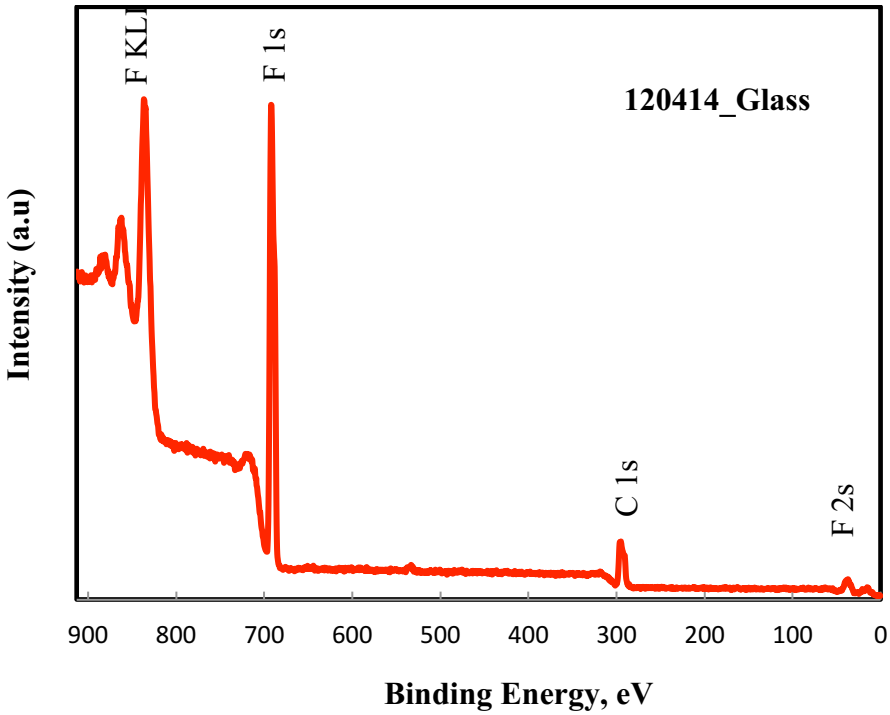

(b)

Figure 28: (a) XPS survey scan of sample 120414 deposited on a silicon substrate, and (b) XPS survey of sample 120414 deposited on a glass substrate.

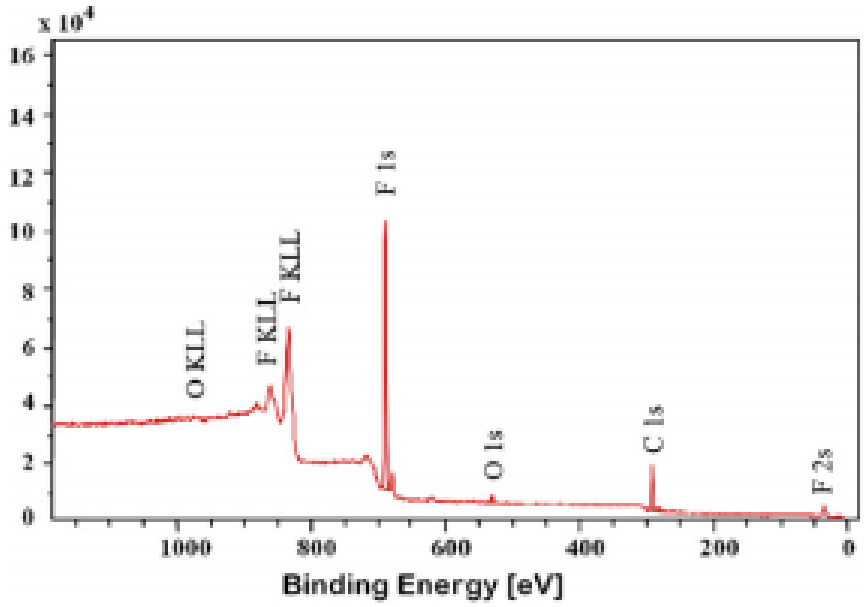

Figure 29: X-ray photoelectron spectroscopy (XPS) survey scan of bulk PTFE [57]

4.3. Scanning Electron Microscopy (SEM) and Energy Dispersive Analysis

Scanning electron microscopy (SEM) was performed on a JEOL JSM 7600F Thermal Field Emission Scanning Electron Microscope by Oxford Instruments equipped with Inca xAct Energy Dispersive Spectrometer (EDX). Due to the nonconductive nature of PTFE thin films, a conducting copper tape was used to avoid charge build up resulting in the destruction of the polymer thin film. SEM images were observed at 2,500 x, 5,000x, and 25, 000x magnification. The electron energy was 2.0 and 4.0 kV with a working distance (WD) of 5.0 mm. Figure 30 shows SEM surface microstructural images of all the 5 samples deposited. Figure 31 shows the cross-sectional images of two samples deposited at two different deposition times. PTFE films were deposited on a silicon substrate at different parameters. From the SEM images, we observe that there exist different microstructures on the surface of the PTFE films.

The microstructure feature observed in Figure 30(a) can be labeled as fractal-like[60]. We observed what can be described as elongated rodlike structures in Figure 30(b) which has a greater degree of anisotropy compared to the other samples. Sample 112014 shows a surface microstructure which can be described as an entanglement of microfibers. These microfibers entanglement form a porous surface layer made of thin PTFE layer of microfibers and intertwined air channels.

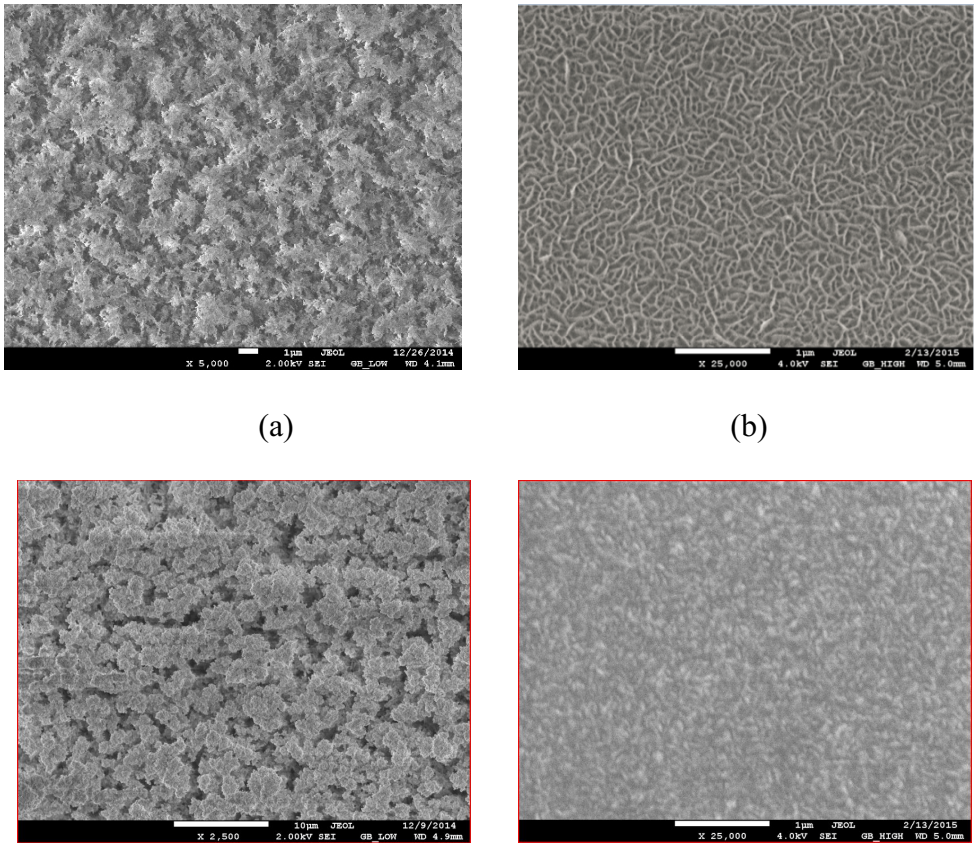

(a) (b)

(c) (d)

Figure 30: SEM micrographs of as deposited iCVD PTFE thin films (a) sample 120414, (b) sample 020915, (c) sample 112014, and (d) sample 020515. All the samples were deposited at different conditions.

SEM cross-sectional images of sample 112014 and sample 120414 are shown in Figure 31. Sample 112014 and sample 120414 were deposited for 25 and 10 minutes respectively. From Figure 30(a), we observe that the average thickness of sample 112014 is 10.78 microns while the average film thickness for sample 120414 is 1.260 microns from Figure 31(b). We note that the thickness of the film increases as the deposition time is increased. This is a parameter that in the future, can be controlled and monitored in real-time with the use of a laser interferometer.

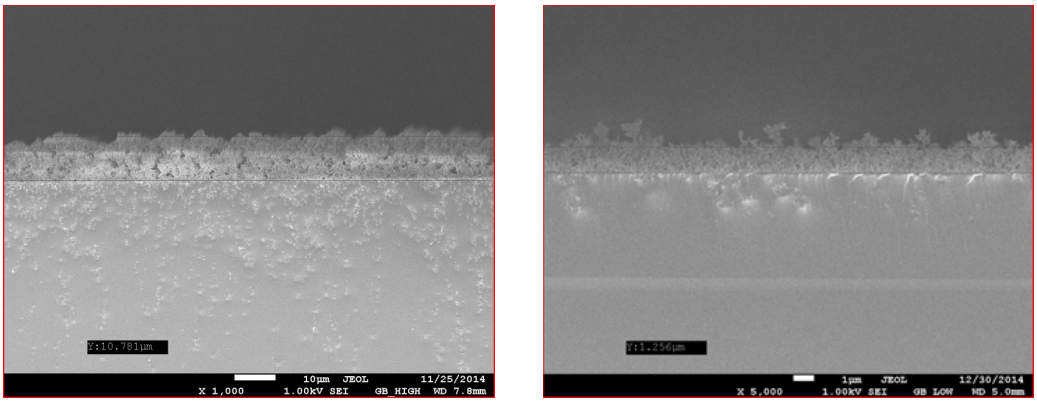

(a) (b)

Figure 31: Cross-sectional SEM micrographs iCVD PTFE thin film showing the thickness of the polymer film (a) sample 112014 deposited for 25 minutes and (b) sample 120414 deposited for 10 minutes.

Table 4 shows different iCVD PTFE samples that were grown at different parameters and deposition times. From the table, we observe that the thickness of the polymer thin film deposited increased with deposition time. Figure 32 shows a plot of film thickness verses deposition time and we note that there is a linear correlation

between the two variables. We observe that as the deposition time is increased, the thickness of the polymer deposited on the substrate increases as well.

Table 4: iCVD deposition times with corresponding film thickness.

Sample ID	Deposition time (mins)	Film Thickness (μm)
112014	25	1.078×10^{1}
120414	10	1.260×10^{0}
011315	5	1.83×10^{-1}
020915	4	1.76×10^{-1}
020515	3	1.10×10^{-1}

EDX analysis was further used to confirm the compositional elements of the iCVD PTFE thin films as shown in Figure 33. Noticeably, from the EDX image below, we observed the presence of carbon (C) and fluorine (F) atoms in the as-deposited iCVD PTFE thin films. We also observe the presence of oxygen in the PTFE film which comes from silicon substrate on which the films were deposited. This could also mean silicon dioxide (SiO_2) layer is present on the surface of the substrate.

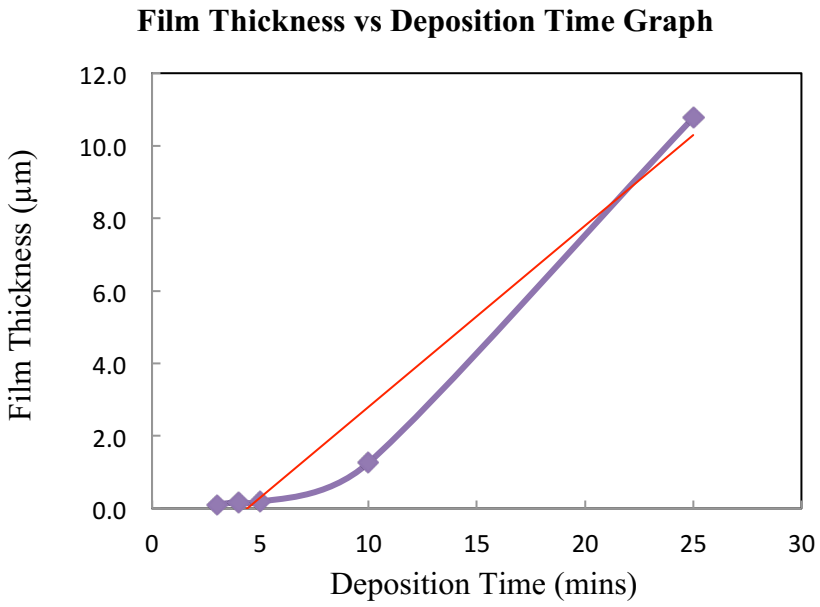

Figure 32: PTFE thin film thickness verses deposition time

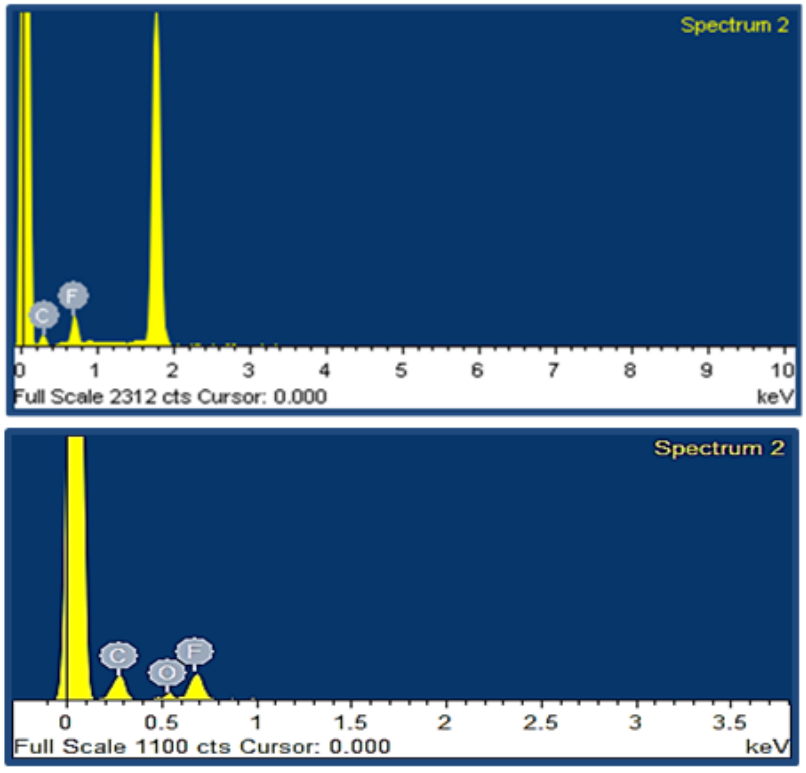

Figure 33: EDX image of sample 011315 (top) and sample 120414 (bottom).

4.4. Atomic Force Microscopy (AFM) Analysis of iCVD PTFE Thin Films

Atomic Force Microscopy (AFM) was done using Veeco Dimension 3100 Nanoscope IIIa Atomic Force Microscope. The surface morphology of iCVD PTFE thin film samples were obtained by AFM in contact mode on a 2 x 2 μm^2 area and shown in Figure 34 (a) - (b). AFM roughness analysis was performed on two iCVD PTFE thin films. In Figure 34(a), we observe anisotropic and grain-like morphology in the iCVD PTFE film deposited at a pressure of between 1.13 and 1.15 Torr and a filament temperature of between 301 and 305˚C. From the iCVD PTFE thin film shown in Figure 34(b) deposited at a pressure of 1.05 ± 0.01 Torr and a filament temperature of between 355 and 360˚C, we see a smoother morphology with nodular structures.

The changes in morphology are associated with the competing nucleation and propagation rates during the iCVD process. Additional AFM images of as-deposited iCVD PTFE thin films are shown in the appendix. Roughness analysis data of three samples are shown in Table 4. From the data, we can observe that the surface roughness decreases with increase in filament temperature and deposition time. Sample 020915_PTFE was deposited at a filament temperature between 301 – 305˚C and has a mean roughness (ra) of 18.059 nm compared to sample 011315_PTFE deposited at filament temperature between 355 – 360 ˚C which has a mean roughness of 10.696 nm.

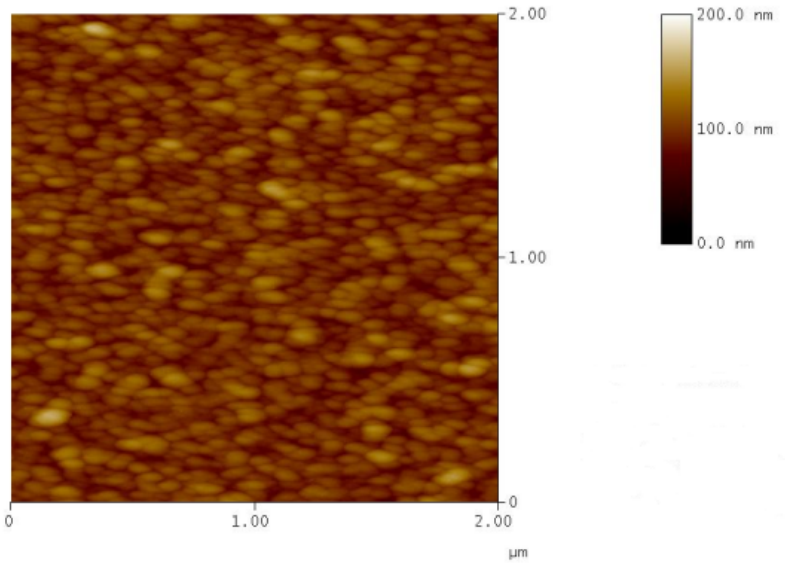

(a)

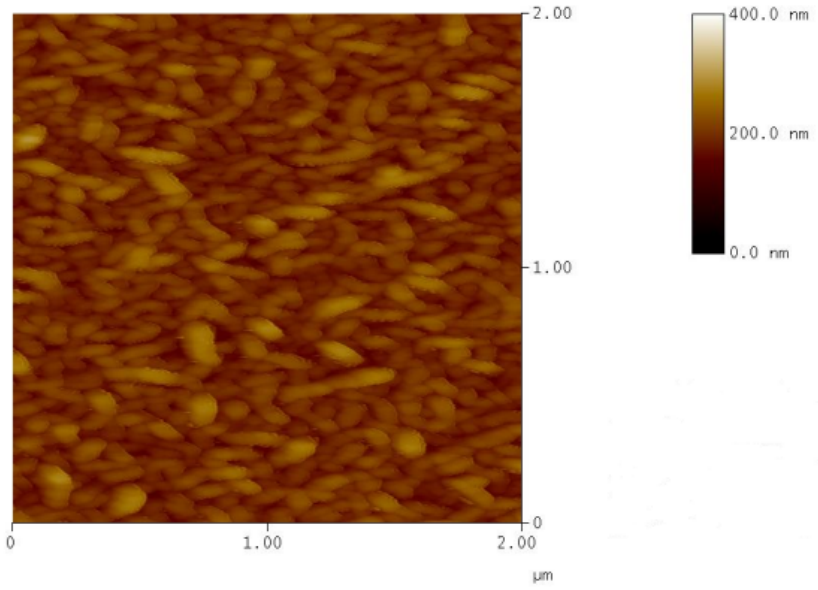

(b)

Figure 34: AFM images of iCVD PTFE thin films deposited at different pressure and deposition time (a) Sample ID 020915_PTFE deposited at 1.1 Torr for 4 minutes and (b) Sample ID 011315_PTFE deposited at 1.05 Torr for 5 minutes. Scan areas are 2 x 2 μm^2.

Table 5: Root Mean Square (RMS) roughness of two iCVD PTFE thin films deposited for two different deposition times.

Sample ID	Mean Roughness (Ra) (nm)	Filament Temperature (˚C)	Deposition time (minutes)
020515_PTFE	2.50	292 - 300	3
020915_PTFE	18.059	301 – 305	4
011315_PTFE	10.696	355 - 360	5

CHAPTER 5: CONCLUSIONS AND FUTURE WORK

5.1: Conclusions

This research work has described the design and construction of custom-built initiated Chemical Vapor Deposition (iCVD) reactor and the deposition of polymer thin film. PTFE thin films were deposited using a relatively new deposition technique known as initiated Chemical Vapor Deposition (iCVD). The iCVD reactor system was custom-built at a low cost. PTFE thin films were deposited under vacuum using perfluoro-1-octanesulfonyl fluoride (PFOSF) as the initiator and hexafluoropropylene oxide (HFPO) as the monomer. The initiator was heated first to vaporize before being metered into the reactor using a needle valves and a set of Swagelok valves. Several parameters such as reactor pressure, filament temperature, filament to substrate distance, and substrate temperature were varied and the results compared. It was observed that in all the runs, PTFE thin films were successfully deposited on the substrate as was confirmed using FTIR and XPS analysis. PTFE thin films deposited using our custom-built iCVD reactor showed active FTIR vibrational modes of linear CF_2 chain structures. From FTIR, we observed that the as-deposited PTFE thin films showed spectra that are characteristically identical to that of bulk PTFE. Furthermore, XPS showed that the PTFE thin films deposited using our custom-built initiated chemical vapor deposited (iCVD) reactor consisted primarily of linear $-(CF2)_n-$ PTFE polymer chains.

iCVD technique has several advantages over other kinds of chemical vapor deposition. In iCVD, thickness of the film is exceedingly controllable. This is because a laser interferometry can be utilized *in situ* to monitor deposition rates and the growth of

the film. With this, real-time film thickness can be monitored and controlled from about 10 nm to several microns. iCVD offers other numerous benefits such as the ability to deposit polymers that are harder to synthesize in solution and eradication of solvents and impurities, as well as the capability of conformal coating on substrates with 3D surfaces and other complex geometries.

Most significantly, the solventless nature of initiated chemical vapor deposition (iCVD) enables deposition of polymer coating with desired properties to substrates of broad collection of morphologies, for instance 3D structures, nanoparticles, a non-planar surfaces and nanofibers. With research tailored in this direction, opportunities to create surfaces with unconventional properties and improvement of device performance are created.

To summarize, this research work pointedly advanced the use of initiated Chemical Vapor Deposition (iCVD) to successfully deposit polytetrafluoroethylene (PTFE) thin films using a custom-built reactor. This can be further improved in the future to make polymer coating that can be used for medical, electrical and other applications in both research and industry.

5.2: Future Work

We have discussed some advantages that our custom-built iCVD reactor possesses over conventional hot-wire Chemical Vapor Deposition, but so far it is not perfect. There were several challenges that were faced during this research and they can be dealt with in the future to obtain even better results. The major challenge that was encountered was accurately controlling the parameters. It was harder to accurately

measure the temperature of the filament and surface substrate. The approach taken was to tape a type K thermocouple probe on a filament and on the side of substrate in order to take temperature reading. This increased the margin of error due to the fact that contact was not good enough and sometime it would be completely detached while the vacuum pump was running

The entire reactor chamber and some parts of the tubing are not completely covered but the heating tape, thus, condensation of the initiator can occur inside the walls of the chamber and the tubing as a result of temperature difference. This problem leads to dramatic decrease in the rate of deposition. Another problem encountered during this research was that needle valves were used to meter both the precursor gas and the initiator into the reaction chamber. Due to this, flow rates of both the monomer and the initiator could not be determined accurately. Without accurate flow rates, it is harder to determine the partial pressures of the initiator and the monomer inside the reaction chamber as well as the total pressure. This problem affects the rate of deposition. In addition, a thermoelectric cooler (TEC) was used to control and maintain substrate temperature close to room temperature. The problem with TEC is that at some time, the colder side became hot and the filament temperature increase. As a result, this affects the adsorption of the monomer and the free radical species on the substrate since it lowers both the sticking coefficient and the rate of deposition of monomer species and free radicals species.

Numerous modifications can be performed in the future to resolve these problems. As future work, the problem of measuring both the filament and substrate temperature can be eliminated with the use of a laser interferometer to measure accurately the

temperatures of both filament array and that of the substrate. Ensuring that the whole reactor chamber is uniformly covered and heated as well as all the tubing will prevent the problem of initiator condensation. Also, using mass flow controllers (MFCs) to meter precursor gas and initiator into the reaction chamber instead of needle valves will allow accurate measurement of flow rates and precise determination of partial pressures. Instead of using TEC to cool the substrate surface, backside water cooling could be used to maintain the temperature of the substrate to avoid the problem of monomer and free radicals desorption from the substrate surface.

REFERENCE

[1]. H. Yasuda, *Plasma Polymerization*. Academic, Orlando, FL, USA, **1985**

[2]. R. Hollahan, A. T. Bell, *Techniques and Application of Plasma Chemistry*. Wiley, New York, NY, USA, **1974**.

[3]. G. H. Yang, E. T. Kang, K. G. Neoh, *J. Polym. Sci. Pol. Chem.* **2000**, *38*, 3498

[4]. S. Zulfiqar, A. Piracha, K. Masud, *Polym. Degrad. Stabil.* **1996**, *52*, 89.

[5]. S. Zulfiqar, M. Zulfiqar, M. Nawaz, I. C. mcNeill, J. G. Gorman, *Polym. Degrad. Stabil.* **1990,** *30,* 195.

[6]. J. W. Lee, E. H. Kim, M. S. Jhon, *Bull Korean Chem. Soc*. **1983***, 4*, 162.

[7]. J. Tamano, S. Hattori, S. Morita, K. Yoneda. *Plasma Chem. Plasma Proc.* **1981,** *1*, 261.

[8]. S. Morita, J. Tamano, S. Hattori, M. Leda. *J. Appl. Phys.* **1980**, *51*, 3938

[9]. M. Yamada, J. Tamano, K. Yoneda, S. Morrita, S. Hattori. *Jpn. J. Appl. Phys. Part 1 – Regul. Pap. Short Notes Rev. Pap* **1982**, *21*, 768.

[10]. L. Martinu, H. Biederman. *Vacuum* **1983**, *33*, 253.

[11]. M. Vasilopoulou, S. Boyatzis, I. Raptis, D. Dimotikalli, P. Argitis. *J. Mater. Chem.* **2004**, *14*, 3312.

[12]. Y. Mao, N. M. Felix, P. T. Nguyen, C. K. Ober, K. K. Gleason. *J. Vac. Sci. Technol. B* **2004**, *22*, 2473.

[13]. L. F. Thompson, C. G. Wilson, M. J. Bowden. *Introduction to Microlithography*, 2nd ed.; Am. Chem. Soc.: Washington, DC, **1994**.

[14]. M. Shirai,, T, Sumino, M. Tsunooka. In Polymeric Materials for Microelectronic Applications: Science and Technology, Ito, H., Tagawa, S., Horie K., Eds.; *Am. Chem. Soc*.: Washington, DC, **1994**; p 185.

[15]. W. H. Teh, C. T. Liang, M. Graham, C. G. *J. Microelectromech. Syst*. **2003,** *12,* 641.

[16].http://fluoroconsultants.com/sitebuildercontent/sitebuilderfiles/introductiontofluoropolymers.pdf

[17]. http://physics.aalto.fi/groups/nanospin/facilities/pulsed-laser-deposition/

[18]. http://groups.ist.utl.pt/rschwarz/rschwarzgroup_files/PLD_files/PLD.htm

[19]. http://www.weizmann.ac.il/materials/igorl/Sputter

[20]. http://www.weizmann.ac.il/materials/igorl/Sputter

[21]. M. J. Ogier, *Bulletin de la société chimique de paris* **1879**, p. 116.

[22]. R. Bakker (2010), *Hot-wire chemical vapor deposition at low substrate temperatures for optoelectronic applications* (Doctoral Dissertation). Retrieved from dspace.library.uu.nl/bitstream/handle/1874/179796/bakker.pdf?...1

[23]. Martin Tech, The microfabrication company, *Reaction Mechanisms of Chemical Vapor Deposition.* Retrieved from http://www.martini-tech.com/reaction-mechanisms-chemical-vapor-deposition/

[24]. S. H. Baxamusa, S. G. In, K. K. Gleason, Initiated and oxidative chemical vapor deposition: a scalable method for conformal and functional polymer films on real substrates, *Phys. Chem. Chem. Phys*., **2009**, *11*, 5227–5240.

[25]. K. Shibuki, M. Yagi, K. Saijo and S. Takatsu, *Surface and Coatings Technology* **1988,** *36***,** 295.

[26]. R. E. I. Schropp, K. F. Feenstra, E. C. Molenbroek, H. Meiling and J. K. Rath, *Philosophical Magazine B: Physics of Condensed Matter; Statistical Mechanics, Electronic, Optical and Magnetic Properties* **1997**, *76,* 309.

[27].S. J. Limb, C. B. Labelle, K. K. Gleason, D. J. Edell, E. F. Gleason, *Appl. Phys. Lett*. **1996**, *68*, 2810.

[25]. H. G. P. Lewis, J. A. Caulfield, K. K. Gleason, *Langmuir* **2001**, 17, 7652

[29]. K. K. S. Lau, K. K. Gleason, *Macromolecules* **2006**, *39*, 3688.

[30]. K. Chan, K. K. Gleason, *Chem. Vap. Deposition* **2005**, *11*, 437.

[31]. Y. Mao, K. K. Gleason, *Langmuir* **2004**, 20, 2484.

[32]. W. E. Tenhaeff, K. K. Gleason: Initiated and Oxidative Chemical Vapor Deposition of Polymeric Thin Films: iCVD and oCVD, *Adv. Funct. Mater*. **2008**, *18*, 979–992

[33]. B. Reejan-Jayan, P. Kovacik, R. Yong, H. Sojoudi, A. Ugur, D. H. Kim, C. D. Petruczok, X. Wang, Andong, L, K. K. Gleason, *Adv. Mater. Interfaces* **2014**, 1, 1400117

[34]. G. Ozaydine-Ince, K. K. Gleason, *J. Vac. Sci. Technol., Surfaces, and Fi*lms **2009**, *27*, 1135.

[34]. K.K., Gleason, H.G. P. Lewis, K. Chan, K.K.S Lau, Y. Mao, *Polymer Nanocoatings by Initiated Chemical Vapor Deposition*, NSTI-Nanotech, **2005**, 2

[36]. http://web.mit.edu/gleason-lab/iCVD.html

[37]. K. K. S. Lau, K. K. Gleason, *Macromolecules* **2006**, *39*, 3688−3694

[38]. K. K. S. Lau, K. K. Gleason. Initiated Chemical Vapor Deposition (iCVD) of poly(alkyl acrylates), A Kinetic Model. *Macromolecules* **2006,** *39*, 3695−3703.

[39]. G. Ozaydin-Ince, A. M. Coclite. K. K. Gleason, *CVD of polymeric thin films: applications in sensors, biotechnology, microelectronics/organic electronics, microfluidics, MEMS, composites and membranes,* Rep. Prog. Phys.75 **2012**, *016501*, 40.

[40]. C. D. Petruczok, N. Chan, K. K. Gleason, Closed Batch Initiated Chemical Vapor Deposition of Ultrathin, Functional, and Conformal Polymer Films, *Langmuir* **2014**, *30*, 4830−4837

[41]. http://www.teamwavelength.com/info/temperaturecontrollers.php

[42]. K. K. Lau, H. G. Pryce Lewis, S. J. Limb, M.C. Kwan, K.K. Gleason, *Hot-wire chemical vapor deposition (HWCVD) of fluorocarbon and organosilicon thin films*, Thin Solid Films **2001**, *395,* 288–291.

[43]. K. K. S. Lau, K. K. Gleason, B. L. Trout, *J. Chem. Phys*. **2000**, *11,* 4103.

[44].http://chemwiki.ucdavis.edu/Physical_Chemistry/Spectroscopy/Vibrational_Spectroscopy/Infrared_Spectroscopy/How_an_FTIR_Spectrometer_Operates, pp 1-11

[45]. *Introduction to Fourier Transform Infrared Spectrometry,* Thermo Nicolet, **2011,** pp 1-7

[46]. http://science.howstuffworks.com/scanning-electron-microscope5.htm, **(2009).**

[47]. http://cmrf.research.uiowa.edu/scanning-electron-microscopy

[48]. M. Misran, *Atomic Force Microscope*, http://www.geocities.ws/misnimisran/AFM07lec.pdf,

[49]. W. Mai, *Fundamental theory of atomic force microscopy*, Professor Zhong L. Wang's nano research group, Georgia Institute of Technology, **2012.**

[50]. S. Wang, J. Li, J. Suo. T. Luo. *Appl. Surf. Sci* **2010,** *256,* 2293.

[51]. G. A. Hishmeh, T. L. barr, A. Sklyarov, S. Hardcastle*, J. vac. Sci. Technol*. A14 1196, 1330.

[52]. B. Bhushan, Y. C. Jung, K. Koch, Philos. *Trans R. Soc.* A367 **2009,** 1631.

[53]. C. Y. Liang, S. Krimm, Infrared spectra of high polymers. III polytetrafluoroethylene and polychlorotrifluoroethylene. *J. Chem. Phys*. **1956,** *25,* 563

[54]. R. Henda, G. Wilson, J. Gray-Munro, O. Alshekhli, A. M. McDonald, Preparation of polytetrafluoroethylene by pulsed electron ablation: Deposition and wettability aspects*. Thin Solid Films*, **2011.**

[55]. L. Li; F. Zi; Y. Zheng: *The characterization of fluorocarbon films on NiTi alloy by magnetron sputtering,* Appl. Surf. Sci., Nov. **2008,** 255, no. 2, pp. 432–434,

[56]. C. Y. Liang, S. Krimm. *J. Chem. Phys.* **1956**, 25, 563

[57]. R. E. Moynihan. *J. Am. Chem, Soc. **1959**,* 81, 1045

[58]. N. P. G. Roeges: *A Guide dto the Complete Interpretation of Infrared Spectra of Organic Structures;* Wiley: New York, **1994.**

[59]. K. K. Gleason. (2015). *CVD Polymers: Fabrication of Organic Surfaces and Devices.* Wiley

[60]. T. Lippert, J. T. Dickinson, *Chemical and spectroscopic aspects of polymer ablation: Special features and novel directions.* Chem. Rev**. 2003**, *103*, 453–486.

APPENDICES

Appendix A: AFM Morphology and Roughness Analysis of iCVD PTFE Thin Films

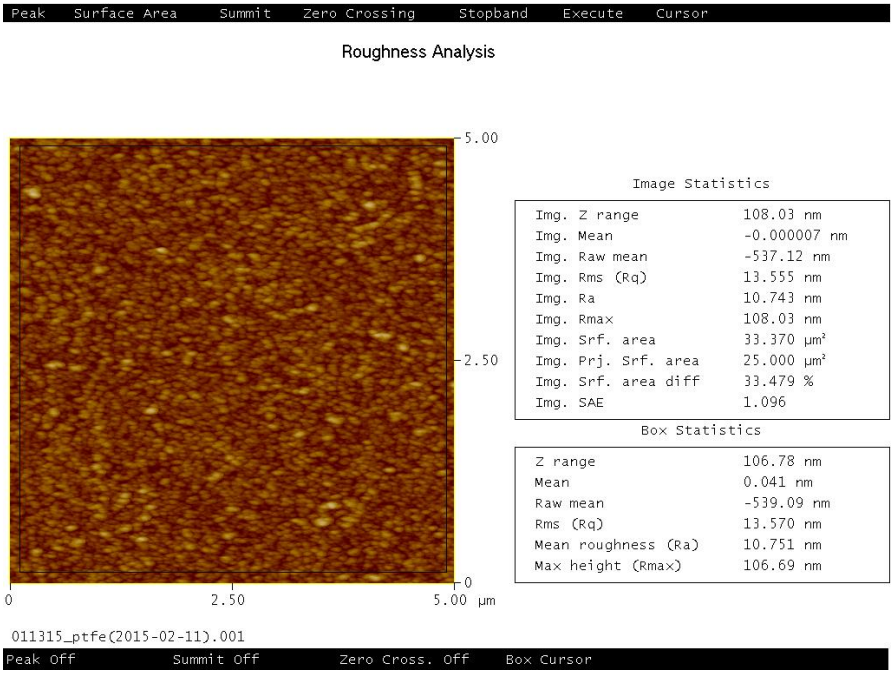

(a)

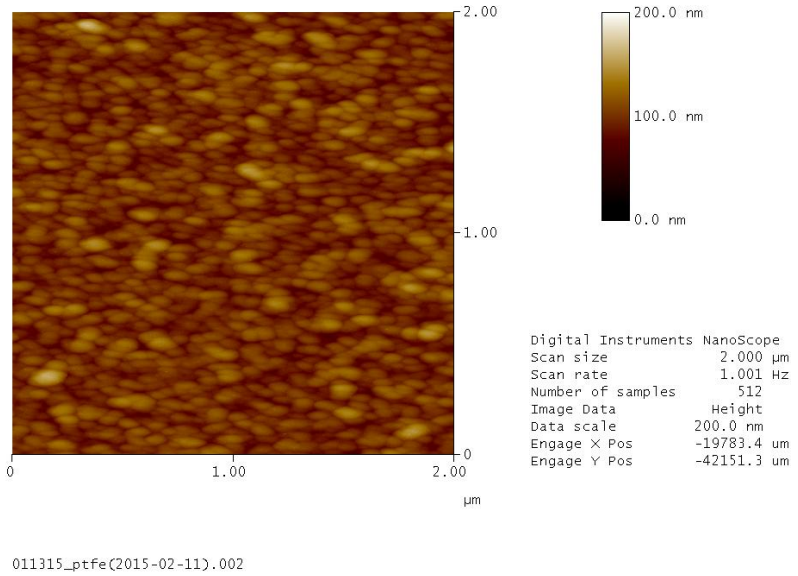

(b)

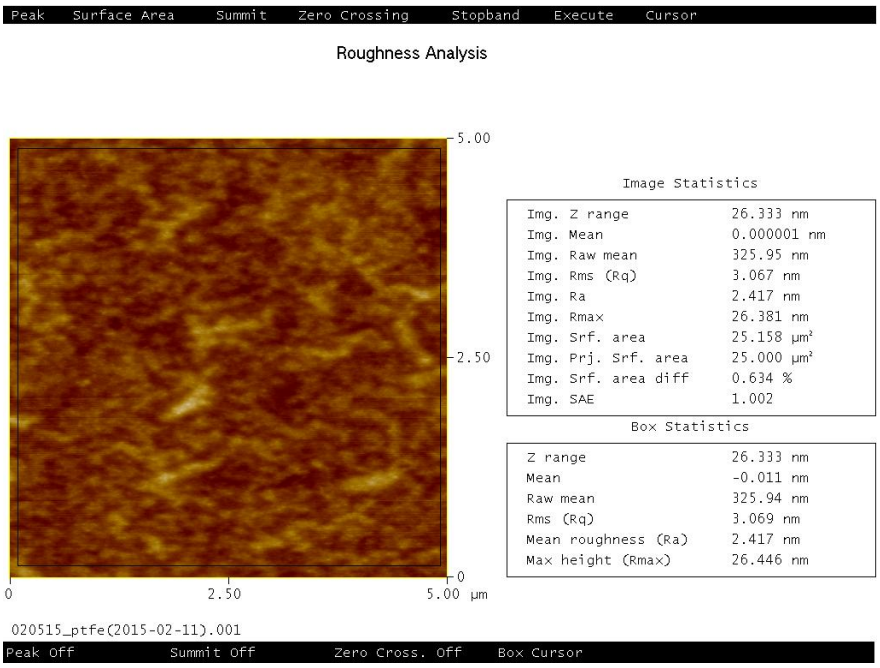
Peak Surface Area Summit Zero Crossing Stopband Execute Cursor
Roughness Analysis
5.00
2.50
0
0
2.50
5.00 µm
Image Statistics
Img. Z range 26.333 nm
Img. Mean 0.000001 nm
Img. Raw mean 325.95 nm
Img. Rms (Rq) 3.067 nm
Img. Ra 2.417 nm
Img. Rmax 26.381 nm
Img. Srf. area 25.158 µm²
Img. Prj. Srf. area 25.000 µm²
Img. Srf. area diff 0.634 %
Img. SAE 1.002
Box Statistics
Z range 26.333 nm
Mean -0.011 nm
Raw mean 325.94 nm
Rms (Rq) 3.069 nm
Mean roughness (Ra) 2.417 nm
Max height (Rmax) 26.446 nm
020515_ptfe(2015-02-11).001
Peak Off Summit Off Zero Cross. Off Box Cursor

(c)

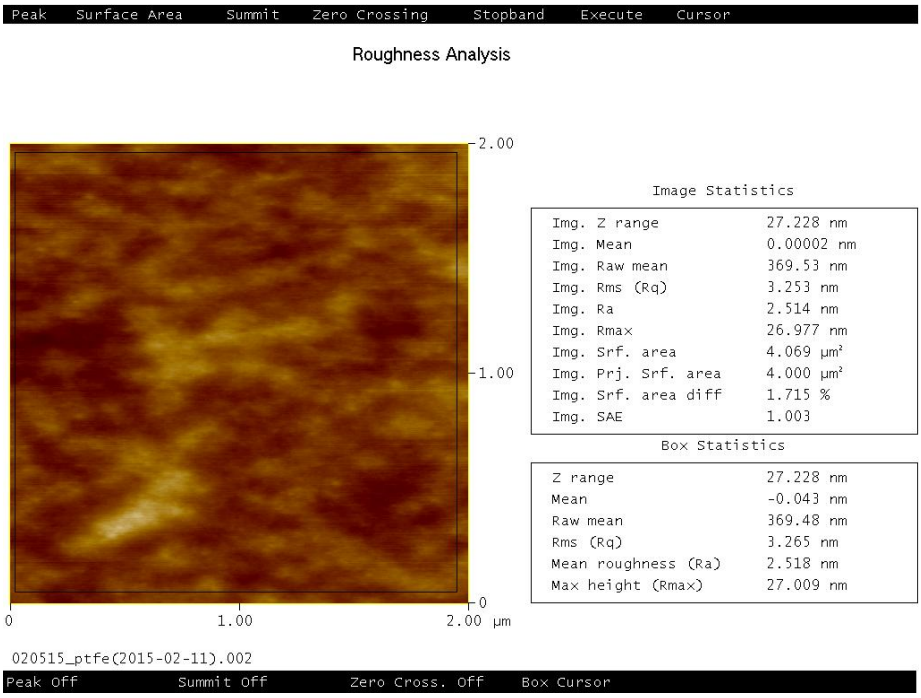
Peak Surface Area Summit Zero Crossing Stopband Execute Cursor
Roughness Analysis
2.00
1.00
0
0
1.00
2.00 µm
Image Statistics
Img. Z range 27.228 nm
Img. Mean 0.00002 nm
Img. Raw mean 369.53 nm
Img. Rms (Rq) 3.253 nm
Img. Ra 2.514 nm
Img. Rmax 26.977 nm
Img. Srf. area 4.069 µm²
Img. Prj. Srf. area 4.000 µm²
Img. Srf. area diff 1.715 %
Img. SAE 1.003
Box Statistics
Z range 27.228 nm
Mean -0.043 nm
Raw mean 369.48 nm
Rms (Rq) 3.265 nm
Mean roughness (Ra) 2.518 nm
Max height (Rmax) 27.009 nm
020515_ptfe(2015-02-11).002
Peak Off Summit Off Zero Cross. Off Box Cursor

(d)

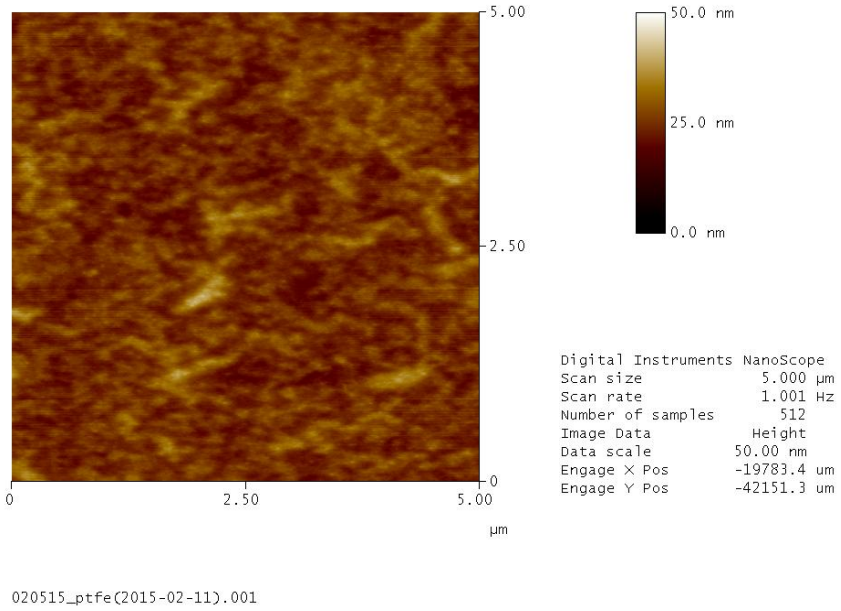

(e)

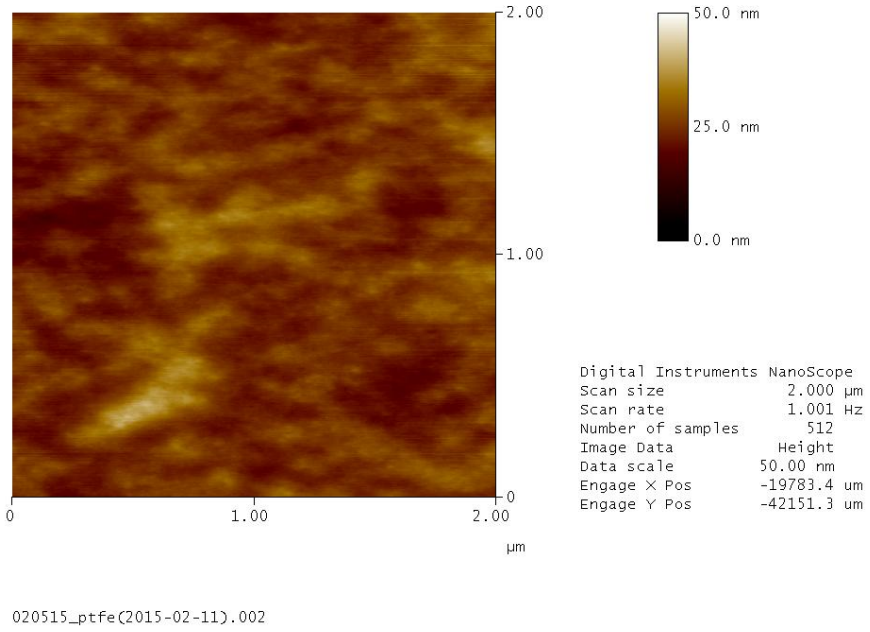

(f)

Additional AFM images showing topographial structure of as deposited iCVD PTFE thin films; sample 011315 a & b, sample 020515 c & d , and sample 020915 e & f.

Appendix B: FTIR Spectra of iCVD PTFE Thin Films

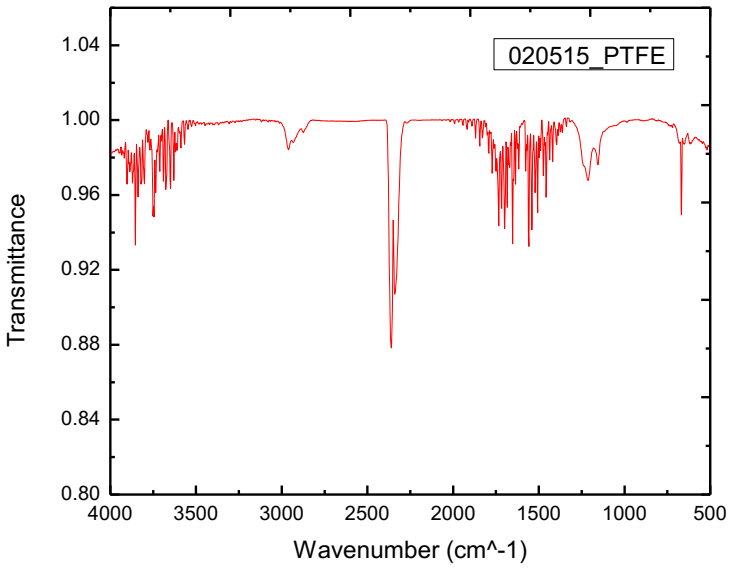

(a)

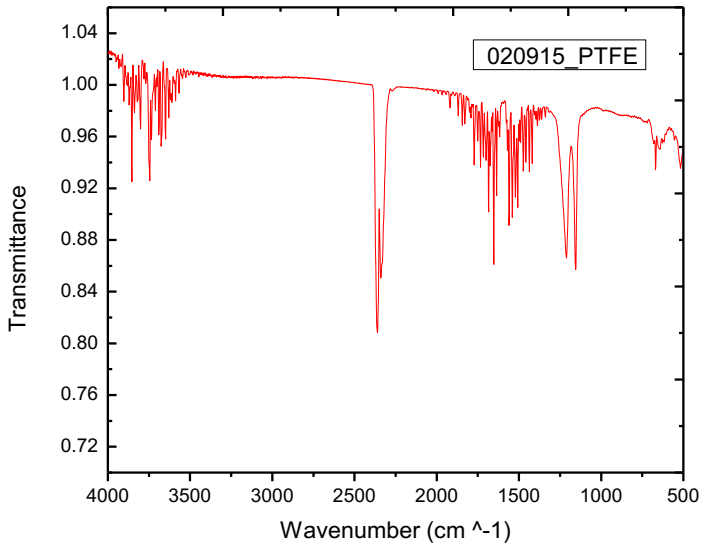

(b)

Additional images of FTIR spectra of as deposited iCVD PFTE thin films (a) sample 02015 and (b) sample 020915.